

Review

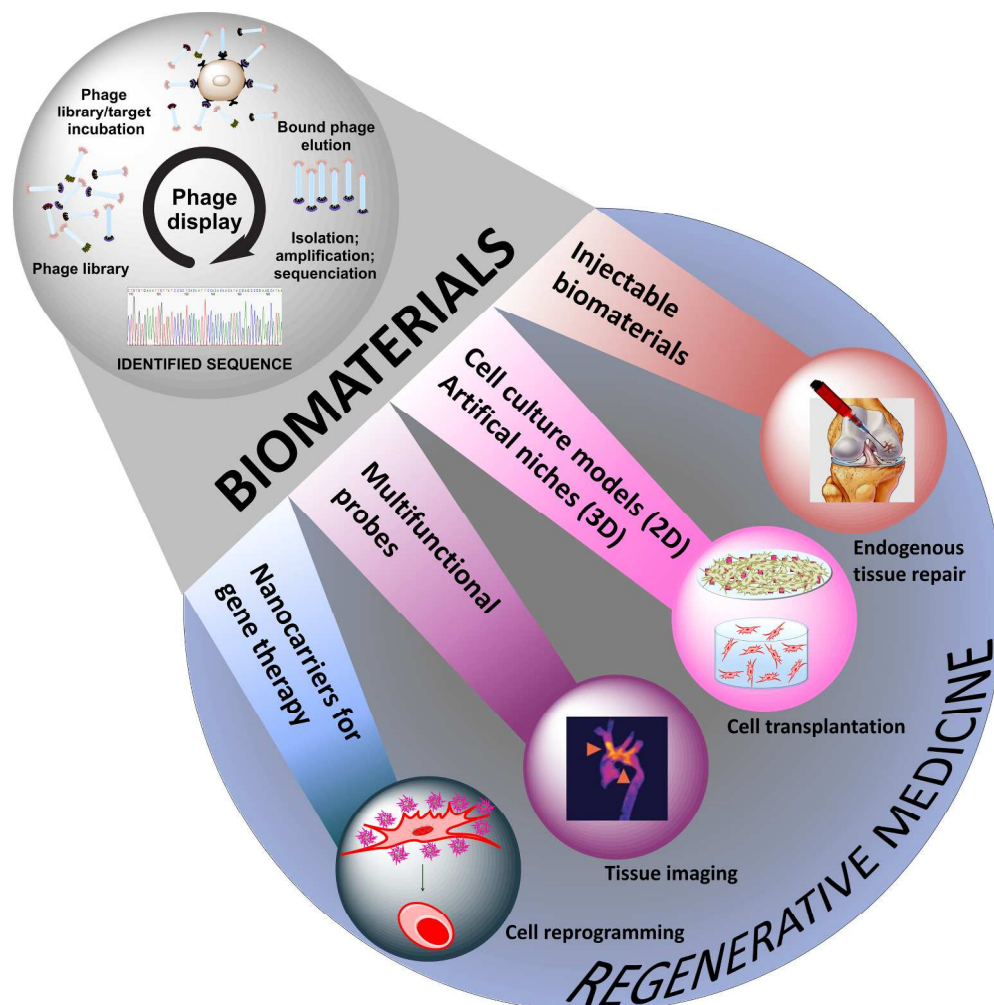
Phage Display Technology in Biomaterials Engineering: Progress and Opportunities for Applications in Regenerative Medicine

Ivone M. Martins, Rui L. Reis, and Helena S. Azevedo

ACS Chem. Biol., **Just Accepted Manuscript** • DOI: 10.1021/acscchembio.5b00717 • Publication Date (Web): 23 Sep 2016Downloaded from <http://pubs.acs.org> on September 23, 2016

Just Accepted

“Just Accepted” manuscripts have been peer-reviewed and accepted for publication. They are posted online prior to technical editing, formatting for publication and author proofing. The American Chemical Society provides “Just Accepted” as a free service to the research community to expedite the dissemination of scientific material as soon as possible after acceptance. “Just Accepted” manuscripts appear in full in PDF format accompanied by an HTML abstract. “Just Accepted” manuscripts have been fully peer reviewed, but should not be considered the official version of record. They are accessible to all readers and citable by the Digital Object Identifier (DOI®). “Just Accepted” is an optional service offered to authors. Therefore, the “Just Accepted” Web site may not include all articles that will be published in the journal. After a manuscript is technically edited and formatted, it will be removed from the “Just Accepted” Web site and published as an ASAP article. Note that technical editing may introduce minor changes to the manuscript text and/or graphics which could affect content, and all legal disclaimers and ethical guidelines that apply to the journal pertain. ACS cannot be held responsible for errors or consequences arising from the use of information contained in these “Just Accepted” manuscripts.



Phage display as a powerful tool to engineer novel biomaterials for diverse regenerative medicine applications.

113x113mm (600 x 600 DPI)

Phage Display Technology in Biomaterials Engineering: Progress and Opportunities for Applications in Regenerative Medicine

Ivone M. Martins^{†, ‡, #} Rui L. Reis,^{†, ‡} Helena S. Azevedo^{†, ‡, §, ¶, *}

[†]3B's Research Group - Biomaterials, Biodegradables and Biomimetics, University of Minho, Headquarters of the European Institute of Excellence on Tissue Engineering and Regenerative Medicine, AvePark, 4805-717 Barco, Guimarães, Portugal

[‡]ICVS/3B's - PT Government Associate Laboratory, Braga/Guimarães, Portugal

[#]CEB – Centre of Biological Engineering, University of Minho, 4710-057, Braga, Portugal

[§]School of Engineering & Materials Science, Queen Mary University of London, London E1 4NS, UK

[¶]Institute of Bioengineering, Queen Mary University of London, London E1 4NS, UK

*Corresponding author

E-mail: h.azevedo@qmul.ac.uk

Tel: +44 (0)20 7882 5502 | Fax: +44 (0)20 7882 3390

ABSTRACT

The field of regenerative medicine has been gaining momentum steadily over the past few years. The emphasis in regenerative medicine is to use various *in-vitro* and *in-vivo* approaches that leverage on the intrinsic healing mechanisms of the body to treat patients with disabling injuries and chronic diseases such as diabetes, osteoarthritis, and degenerative disorders of the cardiovascular and central nervous system.

Phage display has been successfully employed to identify peptide ligands for a wide variety of targets, ranging from relatively small molecules (enzymes, cell receptors) to inorganic, organic, and biological (tissues) materials. Over the last two decades, phage display technology has advanced tremendously and has become a powerful tool in the most varied fields of research, including biotechnology, materials science, cell biology, pharmacology, and diagnostics. The growing interest in and success of phage display libraries is largely due its incredible versatility and practical use. This review discusses the potential of phage display technology in biomaterials engineering for applications in regenerative medicine.

KEYWORDS

Bacteriophages (or phages): viruses that specifically infect bacterial cells and consist of an outer protein capsid enclosing genetic material (dsDNA - vast majority, ssDNA, ssRNA, or dsRNA - very rare, with either circular or linear arrangement).

Biomaterials: synthetic or natural materials designed to interact with tissues and organs in the body to monitor and/or restore their functions.

1
2
3 **Nanotechnology:** technology that involves imaging, measuring, modeling, and manipulating
4 materials on the nanometer scale (i.e. 10^{-9} meter), typically in the range of 1 to 100
5 nanometers.
6

7 **Peptide ligand:** a peptide sequence which binds with high affinity and specificity to a particular
8 target.
9

10 **Phage display panning:** combinatorial process of displaying random peptide sequences or
11 engineered proteins, fused to the coat-proteins on the surface of phages, to identify peptides
12 or proteins (out of billions of candidates) that bind specifically and selectively to a defined or
13 unknown target.
14

15 **Phage display peptide library:** collection of phage particles displaying random peptides
16 containing as many as 10^9 combinations.
17

18 **Regenerative medicine:** new field in the health sciences dedicated to the regeneration of
19 tissues or organs by applying specific cell populations or biomaterial scaffolds, alone or
20 combined, to stimulate the intrinsic healing ability of the body and promote endogenous
21 repair.
22
23

24 **Targeted delivery:** method of delivering a therapeutic (drug, bioactive protein, or gene) or
25 imaging (probe) agent to a specific site in the body, which optimizes its therapeutic or imaging
26 index by restricting its pharmacological or imaging activity to the target tissue or organ, and
27 reducing potential exposure in unwanted sites.
28
29
30
31
32
33
34
35
36
37
38
39
40
41
42
43
44
45
46
47
48
49
50
51
52
53
54
55
56
57
58
59
60

INTRODUCTION

Regenerative medicine (RM) is a growing field of interdisciplinary research and clinical practices that has the potential of transforming the future of healthcare. It seeks to repair or replace malfunctioning cells, tissues, or organs caused by genetic disorders, chronic diseases, injuries or aging (1). It employs a combination of *in-vitro/ex-vivo* and *in-vivo* approaches that may involve transplantation of stem/progenitor, differentiated, or engineered cells, alone or incorporated in biomaterial scaffolds; tissue engineering; and delivery of therapeutic agents (e.g. cytokines, genes, small molecules) for reprogramming cell and tissue types or improving the function of the host environment. All RM strategies leverage on the stimulation of the body's endogenous processes to develop and repair. Accordingly, stem cell research, gene therapy, biomaterials science, and molecular imaging play a central role in RM.

Phage display is a potent, high-throughput technology used for identifying peptide ligands for a given target. The technique applies a library of phage particles displaying an ample variety of peptides or proteins to identify those that bind to a certain target. The utility of this technology derives from phage biology, as phages can be genetically modified to express polypeptides on their surface while the gene encoding the polypeptide, found inside the viral particle, can be analyzed. Since its first establishment by George P. Smith in 1985 (2), phage display has enabled the selection of a vast quantity of different peptides. Although being mostly used to discover peptide ligands for mapping protein–protein interactions, and in the field of antibody engineering, phage display has evolved, now contributing to a variety of different areas of medicine and technology. Some of those areas that now benefit from the system are molecular and imaging diagnosis (3), peptide drug discovery (4), targeted drug and gene delivery (5), vaccine development (6), identification of new receptors and ligands (6), and nanomaterials (7, 8). Several excellent reviews, covering different aspects of phages, including phage biology (9) and the application of phage display in different areas (6, 10–12) have been published.

Cell transplantation often requires prior expansion of the cells *in-vitro* to obtain large numbers of functional cells for clinical applications. Thus *in-vitro* expansion is a critical step in cell-based therapies and typically involves the culture of cells on substrates coated with extracellular matrix (ECM) proteins. However, the batch-to-batch variability of ECM proteins presents limitations for both basic research and clinical applications of stem cells. Phage display technology provides a non-expensive tool for the rapid and efficient screening of peptide ligands on cells or tissues, discriminating between subtle differences in cell surface phenotypes and between normal or diseased tissues. These peptide motifs can be incorporated into biomaterials to guide stem cell proliferation and differentiation *in-vitro* for subsequent transplantation, or to recruit local stem cells *in-vivo* for stimulating tissue regeneration. Using phage-derived peptides targeting specific cells or tissues, rather than the non-specific peptide motifs

1
2
3 routinely used in RM approaches, more controllable and effective regenerative
4 therapies can be developed and tailored to individual patients, leading towards
5 personalized medicine. In addition, phage display can provide novel peptides to
6 investigate peptide–protein interactions that underlie disease mechanisms, which can
7 be further used for designing potential therapeutic agents. Thus, peptide phage display
8 is also a valuable tool in RM, and several therapeutic products generated by this
9 technology are now commercially available (4), demonstrating its clinical potential.
10 This review aims to recount the applications of phage display in biomaterials
11 engineering and RM, highlighting the future of phage display in these fields.
12
13
14
15
16

17 **Phage display screening - biopanning**

18
19 The most common screening method to identify peptide ligands for a given target by
20 phage display (affinity selection) is known as biopanning. This procedure employs a
21 phage display library that consist of a pool of individual clones ($\sim 10^9$) bearing a
22 different foreign DNA insert in the phage genome and presenting a different peptide
23 on its surface. The external gene sequence is merged between genes encoding a signal
24 peptide and a part of the capsid protein, which ensures that the foreign peptide is
25 expressed fused to the coat-proteins. Molecules displayed on phage libraries are not
26 restricted to peptides and antibodies. Random protein fragments, gene fragment- or
27 cDNA-encoded proteins, and mRNA phage display libraries have also been created (13,
28 14), broadening the practical applications of the technology and demonstrating the
29 versatility of the technology.
30
31
32
33

34
35 Typically, the process starts with library exposure to the target of interest to allow
36 binding to the target under suitable conditions. The loosened phages are eliminated by
37 washing, and the remaining bound phages are then eluted for subsequent bacterial
38 infection and amplification. Viral multiplication occurs within the host cells, and
39 thousands of newly-formed phage particles are generated for additional selection
40 rounds (usually 2–5 rounds). After multiple panning rounds, enrichment of target-
41 binding phage is analyzed by phage titering and/or immunological assays. When
42 sufficient enrichment is achieved, single phages are separated and sequenced to
43 identify predominant binding motifs (consensus sequence). Selective clones may be
44 obtained by examining the differences between unselected and selected libraries using
45 DNA sequencing (15, 16).
46
47
48
49

50 Selection of ligands able to distinguish particular features in biological scenarios (cells
51 and tissues) with good specificity and affinity is required for reliable diagnosis and
52 effective regenerative therapies. Thus, potential targets in RM are signaling proteins
53 (e.g. growth factors), cells, and tissues. These targets, however, have many potential
54 binding sites, and non-specific binding to abundant molecules (e.g. albumin) is also
55 believed to affect the outcome of the panning experiments. Hamilton and co-workers
56
57
58
59
60

1
2
3 (17) described the application of phage display to select peptides that bind to bone
4 morphogenetic protein 2 (BMP-2), which is implicated in osteoblast differentiation and
5 stimulates bone formation. Using a recombinant form of human BMP-2 (rhBMP-2),
6 they first biotinylated the protein for immobilization on streptavidin (SA)-coated
7 microtiter plates. Biopanning was performed according to conventional protocols.
8 After 3 cycles of screening, the populations of enriched phages were amplified in
9 bacteria and the binding to BMP-2 was detected by an enzyme linked immunosorbent
10 assay (ELISA).
11
12
13

14 Many studies do not take into account the fact that the high density of receptors at the
15 selection surface does not reproduce the density of receptors present on the native
16 cell membrane. Thus, the binding affinity of the isolated peptide might be lower than
17 the one observed when displayed on the phage. For example, Bastings *et al.* (18)
18 demonstrated, using SA as a model multivalent receptor, that receptor density and
19 ligand valency are important parameters associated with binding strength. They
20 showed that phage affinity for SA-coated surfaces declines significantly into the
21 nanomolar scale when the surface density of SA is reduced. By displaying the peptide
22 ligand in a multivalent arrangement (e.g. dimer, tetramer, or pentameric peptide
23 wedge) they were able to increase (104-fold) the binding affinity as compared to the
24 monovalent peptide. This study suggests that for effective targeting strategies, both
25 the ligand presentation and the density of the corresponding receptor are
26 fundamental aspects to consider. The ligand selection should be conducted on surfaces
27 with physiologically-representative receptor densities, and the peptides identified by
28 phage display should be displayed in an appropriate form (e.g. dendrimer) when
29 engineering biomaterials aiming for successful targeting. In addition, the cell surface
30 contains proteins that can cluster or multimerize, and some of these organization
31 patterns can be disturbed upon preparation of membrane proteins for selective
32 screening. Indeed, the hydrophobic segments of membrane proteins direct them into a
33 lipophilic environment, with such proteins naturally aggregating after separation from
34 the membrane. Recombinant forms of these proteins have been widely used, but
35 recombinant receptors are not always available. Hajduczki *et al.* (19) proposed a new
36 approach for the solubilization and presentation of membrane proteins, by proposing
37 a different strategy for phage display selection. They prepared a phage library
38 displaying caveolin-1 (monotopic membrane protein associated with detergent-
39 insoluble rafts) variants generated by site-directed mutagenesis, and used an anti-
40 selection process, consisting of binding to a hydrophobic resin, to eliminate
41 aggregation-prone hydrophobic variants. The less hydrophobic variants were
42 subsequently recovered and used in positive selection to isolate variants binding to the
43 gp41 ectodomain (a known caveolin function). This additional positive panning
44 ensured that the obtained variants were correctly folded. Thus, phage display
45 screening on whole cells offers more chances to obtain peptides that bind to
46 transmembrane proteins in their natural conformation. Panning on living cells can be
47
48
49
50
51
52
53
54
55
56
57
58
59
60

1
2
3 done either on monolayers of attached cells or on cells in suspension. In these cases,
4 the pool of target-binding phages needs to be diverse, but it can be reduced by
5 performing a negative screening (pre-clearing) on “control” cells (20) or a funnel
6 screening protocol. Kiessling’s group (21) used a screening approach based on the
7 biopanning and rapid analysis for selective interactive ligands (BRASIL) method,
8 previously developed by Giordano and co-workers (20), to isolate peptides binding to
9 the surface of live stem cells. BRASIL is more specific (panning of cells in suspension)
10 and faster than conventional methods that depend on washing or limiting dilution.
11 Because living stem cells present many different receptors on their surfaces, and no
12 appropriate “control cells” were available for a negative selection step, they further
13 optimized the screening to narrow down the pool of cell-binding peptides. They
14 incubated the cells (human embryonal carcinoma cell line) with a mixture (1:1) of
15 peptide-bearing (library) and peptide-free (wild type) phage, and monitored phage
16 titer at each panning and washing step. The phage members that remained bound to
17 cells after all washing stages were then subjected to an additional cycle of incubation
18 and washing, resulting in 50-fold enrichment of the peptide-containing phage.
19 However, many non-specific phages remained in the pool. Therefore, to select the cell-
20 binding phage, they employed another screening step using an ELISA. Seven cell-
21 binding phage clones were isolated from the 370 clones tested.

22
23
24
25
26
27
28
29 Since the human body is made of around 10^{14} cells with distinct types and the surface
30 changes with the state of the cell, the problem gains further complexity *in-vivo*.
31 Although most biopanning experiments are conducted *in-vitro*, it is recognized that the
32 *in-vivo* conditions greatly influences the expression of cell surface molecules, and that
33 the phenotype of certain cells changes when they are cultured *in-vitro*. Thus, the
34 application of phage display selection *in-vivo* circumvents these challenges and allows
35 the identification of ligands able of homing to specific tissues or organs (6, 22-25). In
36 order to achieve this process, phage libraries are injected intravenously into animals
37 and allowed to circulate for a certain time. While nonspecific phages tend to be found
38 throughout the whole organism, phages with selective binding will concentrate in
39 certain tissues or organs. The bound phages are recovered and amplified and their
40 DNA is sequenced. Pasqualini and Ruoslahti (24) were the first to report this approach,
41 isolating peptides that home to renal and cerebral vascular endothelium *in-vivo*. *In-*
42 *vivo* panning has also been applied to identify peptide ligands with potential
43 applications in RM. For example, Nowakowski *et al.* (26) were the first to conduct a
44 phage display experiment involving the bone marrow and stem cells. They injected the
45 phage display library into the tail vein of mice and, 10 minutes after injection, isolated
46 the bone marrow to elute phages bound to bone marrow cells. The eluted phages
47 were purified, amplified, and then reinjected. Five rounds of screening resulted in the
48 identification of a peptide that preferentially homes to bone marrow, also binding to
49 resident hematopoietic stem cells. The receptor of this peptide may be involved in
50 bone marrow engraftment by recruiting hematopoietic stem cells.
51
52
53
54
55
56
57
58
59
60

1
2
3 One of the most laborious and costly steps (rate-limiting) in phage display screening is
4 the DNA sequencing of the encoded displayed peptides. Next generation sequencing
5 (NGS), such as Illumina deep sequencing technology, permits a high-throughput and
6 cost-competitive phage display selection because it can characterize over 10^7 reads in
7 a single run, providing more complete coverage of the libraries (27). This is particularly
8 useful for panning on RM targets such as cells, which present hundreds of different
9 receptors. For example, Hoen and colleagues (28) applied NGS to analyze the phage
10 library at different stages of the selection process when panning on KS483 osteoblast
11 cells, finding positive hits after one round of selection. Since its first application, NGS
12 has been applied to enhance phage display protocols (28-31), allowing the isolation of
13 phage binders after the first biopanning round, and the selection of less frequent but
14 more specific peptides. As an example, a new method for selection against targets
15 located on the cell surface, which are less abundant and cannot be purified, was
16 implemented by the Lerner lab (32). This method allows for the identification of
17 ligands for less-fit molecules with lower affinity. Having ligands with lower affinity can
18 be useful for neutralizing the function/activity of the target through binding to
19 different regions.
20
21

22
23
24
25
26 In the following sections, we describe applications of phage-derived peptides in the
27 functionalization of novel biomaterials with potential implications in RM strategies.
28
29
30

31 **APPLICATIONS OF PHAGE DISPLAY IN BIOMATERIALS ENGINEERING FOR** 32 **REGENERATIVE MEDICINE** 33

34 The advances in phage display have greatly expanded the applications of the
35 technology, creating new opportunities in biomaterials engineering and RM. Figure 1
36 shows examples of *in-vitro* and *in-vivo* RM strategies using different biomaterial
37 systems functionalized with peptides identified by phage display. Phage-derived
38 peptides, able to bind specifically to receptors on the surface of stem cells, can be used
39 to functionalize synthetic scaffolds (2D surfaces and 3D hydrogels) for promoting stem
40 cell expansion (Figure 1-a) or differentiation (Figure 1-b) *in-vitro*. *In-vivo* approaches
41 include the incorporation of peptide ligands identified by phage display into injectable
42 biomaterials (e.g. nanofibers), which can bind to growth factors (GFs) and promote
43 endogenous tissue repair (Figure 1-c), or into nanobiomaterials (e.g. liposomes,
44 dendrimers), which can bind to receptors on the cell surface and deliver genetic
45 material to target cells (gene therapy, Figure 1-d).
46
47
48
49
50
51
52
53
54
55
56
57
58
59
60

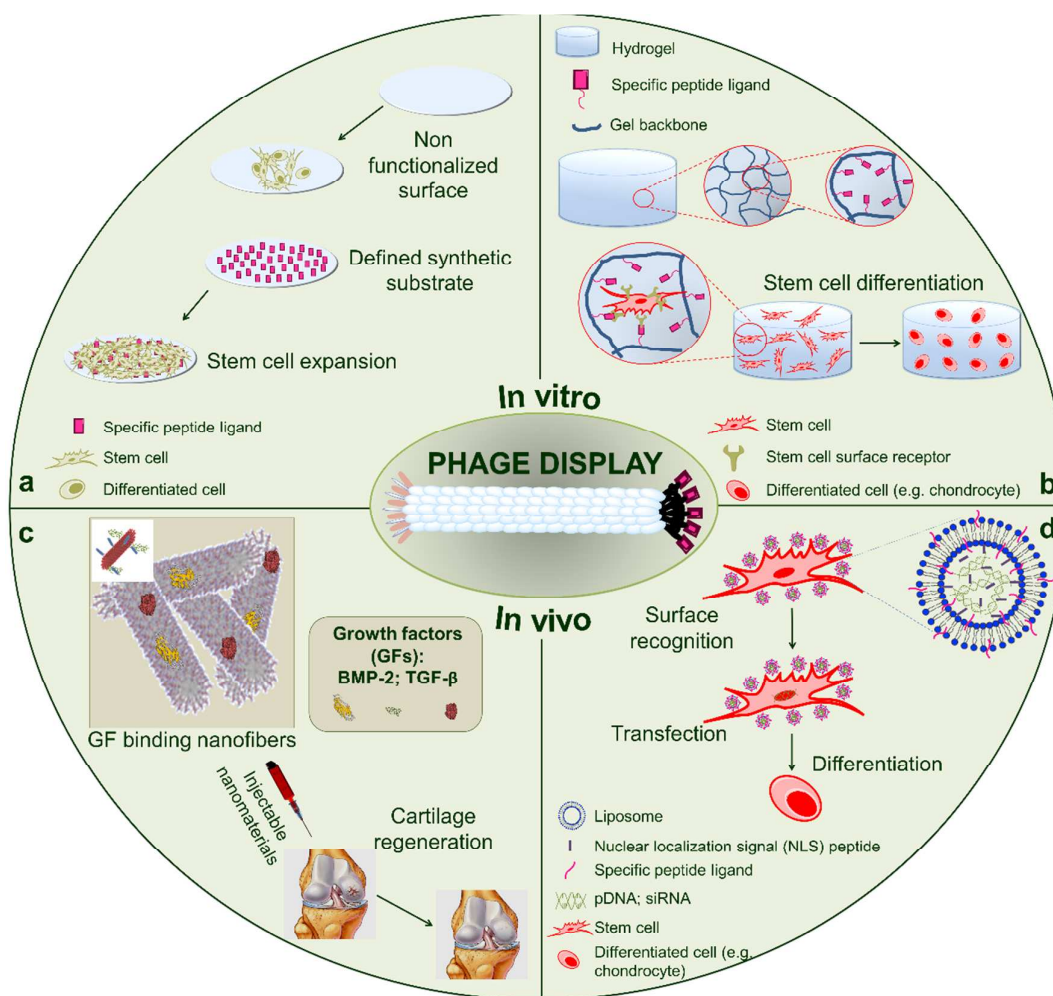


Figure 1. The use of phage display (center: M13 phage displaying a random peptide library on coat-protein 3) in biomaterials engineering and their applications in *in-vitro* (a, b) and *in-vivo* (c, d) RM approaches. (a) Functionalized synthetic substrates (2D surfaces) for stem cell expansion; (b) Functionalized hydrogels (3D environments) for recreating/manipulating stem cell niches; (c) Functionalized injectable biomaterials for sequestering GFs to promote endogenous tissue repair; (d) Functionalized nanocarriers for cell reprogramming (target delivery of genetic material to specific cells).

Different databases (PepBank, Tree of Medicine, BDB) collating peptide sequences identified by phage display can be accessed free of charge, greatly contributing to data mining in this area. Currently, the biopanning data bank (BDB, at <http://immunet.cn/bdb/>) formerly known as MimoDB (33, 34) contains 26813 peptide sequences, showing that the use of phage display has exploded over recent decades. However, many of the discovered sequences have not been further analyzed and validated *in-vitro* or *in-vivo* to assess specificity, selectivity, and stability, nor have they had their structure optimized to be clinically useful. To facilitate the search of sequences with utility for RM applications, we have compiled in Table 1 a selected list of peptide sequences that bind to RM targets (i.e., ECM components of tissues, GFs, surface of stem and differentiated cells). These peptide ligands can be used to specifically localize imaging probes or drugs to damaged tissues for diagnostic

1
2
3 (immunohistochemistry, magnetic resonance imaging, positron emission tomography)
4 and therapeutic (treating diseases) purposes; to deliver different biologics (e.g., GFs,
5 oligonucleotides) to selected cell types for controlling their behavior (adhesion,
6 survival, proliferation, migration, differentiation, angiogenesis); or to recruit local stem
7 cells to sites of injury for stimulating tissue regeneration. The BiopanningDataSet ID
8 was also included, when available, to facilitate the search in MDB, as well as the
9 equilibrium dissociation constant (K_D), which represents the binding affinity between
10 the peptide ligand and the target, or the half inhibitory concentration (IC_{50}) from
11 competition binding assays. In addition, a follow-up was performed to identify
12 transformative publications that have identified breakthrough sequences, inspired new
13 experiments based on the original sequence, and contributed to their application and
14 clinical development, with potential impact on RM. To discriminate such contributions,
15 quantitative data on the number of citations for each publication were first gathered,
16 and from these, original articles were selected (excluding reviews, editorials, book
17 chapters) to perform the analysis. While carrying out this evaluation, we must bear in
18 mind that, typically, there is a 1–3 year citation lag time for each article with impact,
19 and certain sequences have been only recently published. Table 1 also summarizes the
20 outcome of this analysis by identifying the number of publications that describe
21 subsequent use of the original peptide sequence in diverse experimental studies,
22 including *in-vitro* and *in-vivo* testing/characterization, and optimization/formulation
23 toward their medical application. More details on this analysis can be found in Table S1
24 (supplementary information). Many of the listed sequences have not resulted in any
25 follow-up papers, mainly because they have been only recently discovered (since
26 2008). One exception is compstatin, a cyclic tridecapeptide first identified by Sahu (35)
27 from phage-display libraries, which binds to complement component 3 (C3), a protein
28 of the immune system. An excellent review on the “clinical trajectory” of compstatin
29 was provided by Ricklin and Lambris (36). This peptide has contributed significantly to
30 the understanding of compstatin–C3 interactions and the generation of new
31 therapeutics (complement inhibitors). Compstatin, and in particular POT-4 (Table S1),
32 which has been commercialized by Potentia Pharmaceuticals, Inc., has entered phase I
33 clinical trials for the treatment of age-related macular degeneration, and can be used
34 for biomaterial functionalization to inhibit biomaterial-induced complement activation
35 (37).
36
37
38
39
40
41
42
43
44
45
46
47
48
49
50
51
52
53
54
55
56
57
58
59
60

Table 1 Selected peptide sequences identified by phage display that bind to targets with relevance for biomaterials engineering in regenerative medicine applications									
	Target	Sequence (<i>BiopanningDataSet ID</i>)	Ref. ^a (year)	K _D (μM)	Designation/ Commercial name	Follow-up ^b			
						Char ^c	Opt ^d	Appl ^e	
ECM components	Collagen (col)	Col I (rat)	HVWMQAP (38) (2009)	61±5	Col I binding peptide	-	-	1	
		Col I (human) (demineralized bone matrix)	SWWGFWNGSAAPVWSR (39) (2008)	<0.1 (EC ₅₀)	-	-	-	1	
		Col II (bovine cartilage grafts)	WYRGRL (486) (2008)	0.14 (IC ₅₀)	Col II binding peptide	-	-	5	
		Col IV (human)	KLWVLPK (41) (2010)	0.114 (IC ₅₀)	-	-	-	5	
		Hyaluronan (HA)	GAHWQFNALTVR (756) (2000)	1.65	HA-binding peptide Pep-1	1	2	23	
	Hydroxyapatite (HAP)	Crystalline HAP	SVSVMKPSRP (43) (2008)	14.1±3.8	-	3	-	1	
		Synthetic HAP powder	MLPHHGA, NPGFAQA (44) (2008)	ND	-	-	1	2	
		Single crystal HAP (100)	NPYHPTIPQSVH (1342) (2011)	ND	-	-	-	1	
	Cell surface, tissues and organelles	Differentiated cells	Cardiomyocytes	QPFTTSLTPPAR (1883) (2011)	ND	-	-	-	-
			Chondrocytes <i>Mouse</i>	RLDPTSYLRTFW, HDSQLEALIKFM (2167) (2013)	ND	-	-	-	-
<i>Rabbit</i>			DWRVIIPRPSA (1549) (2011)	ND	CAP (chondrocyte affinity peptide)	-	-	1	
Stem cells		Adipose derived							
		Human adipose stem cells (ASCs)	MLAGWIP (1576) (2008)	ND	-	-	-	-	
		Mouse ASCs	SWKYWFGE (1552), WLGEWLG (1576) (2011)	ND	WAT7	-	-	-	
		Bone marrow derived							
		Human mesenchymal stem cells (MSCs)	EPLQLKM (1941) (2012)	ND	E7 (hBMMSC affinity peptide)	-	-	5	
		Mouse MSCs	NSMIAHNKTRMH (52) (2008)	ND	LAB (low affinity binding) peptide	-	-	1	
			SGHQLLLNKMPN (26) (2004)	ND	HAB (high affinity binding) peptide	-	-	1	
		Murine MSCs	STFTKSP (682) (2004)	ND	BMHP (bone marrow homing peptide)	2	-	4	
		Rat MSCs	VTAMEPGQ (2294) (2013)	ND	-	-	-	2	
		Embryonic derived							
		Human embryonic stem cells (ESCs) cell line X-01	HGAAWGTRTGHV (54) (2013)	ND	H166	-	-	-	
		Human ESCs	VGGEAWSSPTDL (21) (2010)	ND	H178	-	-	-	
	TVKHRPDALHPQ, LTTAPKLPKVTR (2010)	ND	-	-	1	-			

		(655)						
	Mouse ESCs	KHMHWHPPALNT (1262)	(55) (2010)	≈ 0.8 (IC ₅₀)	Seq2 peptide	-	-	-
	Rhesus macaque ESCs	APWHLSSQYSRT	(56) (2010)	≈ 0.5 (IC ₅₀)	-	-	-	-
	Neuronal derived							
	Mice neuronal precursor cells (NPCs)	QTRFLLH, VPTQSSG	(57) (2007)	(0.3 μg) (IC ₅₀)	-	-	-	1
	Murine neuronal stem cells (NSCs)	KLPGWSG (2240)	(58) (2013)	ND	KLPGWSG peptide	1	-	-
	Rhesus monkey NSCs derived from ES cell line RS366.4	HGEVPRFHAVHL (1516)	(59) (2010)	≈ 0.5 (IC ₅₀)	HGE peptide	-	-	-
	Porcine skin	TGSTQHQ (1847)	(60) (2011)	ND	SPACE (skin permeating and cell entering) peptide	-	-	5
	Human Kaposi sarcoma KS1767 cell line (mitochondria/endoplasmic reticulum fraction)	YKWYYRGAA	(61) (2012)	ND	-	-	-	1
Growth factors	Bone morphogenetic protein 2 (BMP-2)	TSPHVPY	(62) (2005)	0.037	-	-	-	2
	rhBMP-2	AGAWAEFSSLSGSRV	(17) (2013)	0.0014 (EC ₅₀)	BC-1	-	-	-
	Human recombinant basic fibroblast GF (rhbFGF)	RTGQYK	(63) (1993)	0.122	-	1	-	2
	Transforming GF β-1 (TGFβ-1)	HSNGLPL	(62) (2005)	ND	-	-	-	3
Cell receptors	Human recombinant stabilin-2 (4e5 domain)	RTLTVRK	(64) (2011)	ND	S2P (stabilin-2 peptide)	-	-	-
	TGF-βR (human extracellular domain of TβRI and TβRII)	LTGKNFPMFHRN	(65) (2010)	≈ 10	Pep1	-	1	-
		MHRMPSFLPTTL (1250)	(65) (2010)	≈ 10	Pep2	-	1	-
	rhTGF-β sRII/Fc	GLLPVGRPDRNVWRWL KGQCDFKGLPEW	(66) (2002)	≈ 1	-	-	-	-
Other proteins	Complement 3 (C3)	ICVVQDWGHRCT (<i>cyclic peptide</i>)	(35) (1996)	ND	Complement-inhibiting peptide Compstatin	10	21	19
	Vascular cell adhesion molecule 1 (VCAM-1)	VHSPNKK (354)	(67) (2005)	ND	Cyclic VCAM-1 peptide, known as VP (<i>in-vitro</i> screening)	-	3	2
		VHPKQHR (353)	(68) (2006)	30	Linear VCAM-1 internalizing peptide-28 (VINP ₂₈) (<i>in-vivo</i> screening)	-	-	12

^a Reference/Year when the sequence was reported for the first time; ^b Number of research papers, from Web of Science Core Collection (Thomson Reuters), that describe subsequent use of the original sequence. Please see Table S1 for more details; ^c Characterization (determination of binding affinity, activity, stability, safety); ^d Optimization (rational, combinatorial and computational optimization to

1
2
3 design new analogues with improved affinity/activity); ^e Application (biomaterials engineering for
4 targeted binding/delivery, conjugation with imaging agents for targeted detection, mechanistic studies
5 and therapeutics); ND: not determined.
6

7
8 In some cases, more than one sequence is identified for the same target. For example,
9 when screening hydroxyapatite (HAP) materials, different powder particles, of various
10 sizes and morphologies, used for the selection may explain the observed differences.
11 Ideally, the selection should be performed using a material with specific morphology,
12 crystallography, and stereochemistry. As described previously, several phage clones
13 are selected in a first screening, and the relative affinity tends to increase with an
14 increasing number of panning cycles. After this first screening, isolated clones are
15 analyzed by ELISA, for example, for cross reactivity and binding ability. Sequences with
16 varied affinities (high, intermediate, or low binding constants) can be obtained, thus
17 allowing the engineering of binding affinity and specificity. Furthermore, by comparing
18 the sequences obtained by phage display with the ones derived from natural proteins
19 known to bind to the same targets, differences in the amino acid composition and
20 sequence are also observed. For example, Mummert *et al.* (42) found a 12-mer peptide
21 that binds to hyaluronan (HA, Table 1) using phage display. This peptide sequence does
22 not show significant (>25%) similarity with the HA-binding motifs found in hyaladherins
23 (CD44, RHAMM, or link protein) (69), nor does it shows a consensus domain, known to
24 be identical among these three HA-binding proteins (69). Nonetheless, the authors
25 showed that the phage-identified peptide specifically binds to HA free in solution or
26 bound to a substrate, and also to HA expressed on the cell surface, and that prevented
27 the binding of HA to leukocytes and their attachment to HA coated surfaces. In
28 addition, this sequence has been validated in numerous subsequent studies (Table S1).
29
30
31
32
33
34
35
36
37

38 **Biomaterials functionalized with peptide ligands identified by phage display as *in-*** 39 ***vitro* cell culture models**

40
41 The isolation and culture of human stem cells *in-vitro* have largely contributed to
42 important advances in fundamental cell biology and cell therapies, by understanding
43 the molecular mechanisms involved in the processes by which stem cells undergo self-
44 renewal or differentiation (70). Recent discoveries have shown novel mechanisms by
45 which stem cell fate is regulated (71-73), but continued research in the molecular
46 biology of stem cells will boost their application in RM. A challenge in cell-based
47 therapies is to find adequate sources of stem cells and the need for maintaining them
48 undifferentiated during *in-vitro* expansion. Thus, there is an urgent need to develop
49 precise and reproducible culturing systems able to control the behavior of human stem
50 cells *in-vitro*. In addition, for cell therapies in humans, an essential requirement is to
51 avoid the exposure of stem cells to animal-derived components during culture.
52 Advances in biomaterials engineering has enabled the development of *in-vitro* culture
53 platforms for cell expansion, and also for the differentiation of stem cells into specific
54
55
56
57
58
59
60

1
2
3 lineages. *In-vivo*, cells receive signals from the ECM and other cells through specialized
4 transmembrane proteins that bind to components of the ECM and receptors of
5 neighboring cells. One potential approach to mimic these interactions and guide cell
6 growth or differentiation *in-vitro* is the use of biomaterials based on peptide
7 sequences that bind to those cell receptors. Phage display has been applied to probe
8 the surface of different stem cells, including adipose progenitor cells (49, 50), bone
9 marrow-derived mesenchymal stem cells (MSCs) (26, 51-53, 74), and embryonic stem
10 cells (ESCs) (21, 54-56) (Table 1). The latter are of special interest, considering their
11 differentiation pluripotency. Peptide ligands for stem cell receptors can then be
12 broadly used in cell culture and differentiation (immobilized on 2D surfaces or 3D
13 hydrogels), namely, as probes for detection of specific stem cell populations during
14 isolation procedures or to ascertain the role of proteins for stem cell differentiation.
15
16
17
18
19
20

21 ***2D substrates for the controlled expansion (and/or differentiation) of (stem) cells***

22
23
24 Kiessling and collaborators (21) used a peptide sequence identified by phage display
25 (binding receptors on human embryonal carcinoma, Table 1) for culturing ESCs. Using
26 self-assembled monolayers (SAMs) for displaying bound peptide ligands on a synthetic
27 surface (Figure 2-a1), they showed that these chemically defined functional substrates
28 supported the undifferentiated proliferation of pluripotent cells (Figure 2-a2). These
29 cells are capable of replicating indefinitely and generate all human cell types, offering a
30 useful resource for both research and RM. Thus, a surface with a well-defined
31 composition could eliminate the problem associated with the use of animal-derived
32 proteins, which suffer from batch-to-batch variability, and increase the predictability of
33 culturing cells *in-vitro*.
34
35
36

37
38 Similarly, MSCs cultured on peptide SAMs containing BMHP1 (Table 1, Figure 2-b1) in
39 maintenance medium (DMEM) or osteogenic differentiation medium (ODM) were able
40 to produce higher amounts of calcium than when cultured on bare substrates (Figure
41 2-b2, b3), demonstrating that BMHP1 can enhance cell mineralization. It was also
42 shown that the amount of calcium deposition was dependent on the peptide density
43 (Figure 2-b3).
44

45
46 These studies showed the utility of the identified peptides for elucidating cell–matrix
47 interactions in 2D. This information could be translated for the functionalization of 3D
48 biomaterials to control cell behavior.
49
50
51
52
53
54
55
56
57
58
59
60

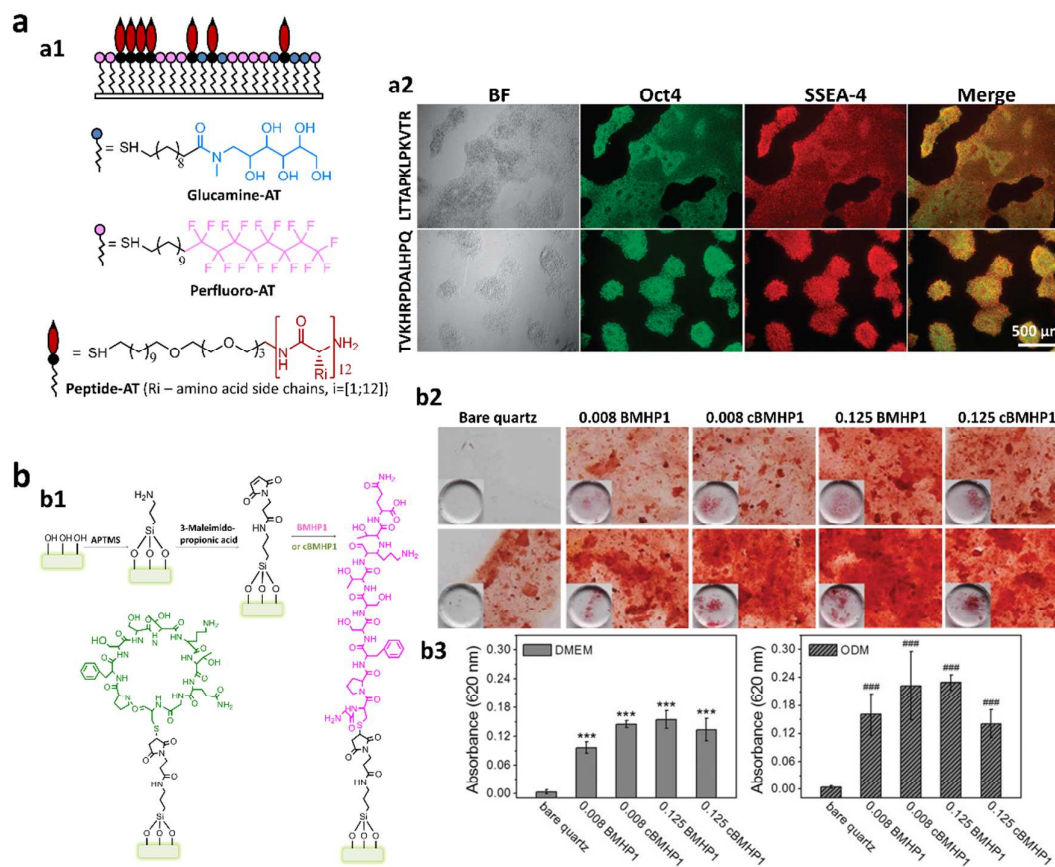


Figure 2. 2D biomaterials (surfaces) functionalized with peptide sequences identified by phage display for *in-vitro* cell culture (proliferation and differentiation). (a) Synthetic surfaces of SAMs displaying phage-derived peptides that bind to the surface of human ESCs support their undifferentiated growth; (a1) SAMs composed of perfluorinated alkanethiols (ATs) containing different ratios of peptide-AT and glucamine-AT (non-adherent for cells) to obtain surface arrays of peptides with different densities; (a2) Human ESCs (hESCs) proliferating on peptide-AT SAMs maintain expression of markers of pluripotency (Oct4 and SSEA4). Adapted with permission from ref. (21). Copyright 2010 American Chemical Society. (b) BMHP1 immobilized on 2D surfaces induce the osteogenic differentiation of MSCs; (b1) Linear and cyclic BMHP1 (cBMHP1) were conjugated to maleimide-functionalized quartz substrates *via* a cysteine residue inserted in the N-terminal; (b2) Low-magnification (200 \times) inverted microscopy images of Alizarin Red S (forms a bright red complex with calcium) staining on MSCs cultured on bare and peptide-functionalized surfaces in DMEM (top panel) and ODM (bottom panel) for 7 days (insets show macroscopic images); (b3) Colorimetric quantification of calcium deposition by cells cultured in DMEM (left) and ODM (right). Adapted from ref. (75) with permission of The Royal Society of Chemistry.

Growth factors (GFs) are involved in numerous cellular processes, such as cell growth, differentiation, and migration. TGF- β is able to both positively and negatively affect inflammation and wound healing. Thus, several studies have been performed towards the identification of peptide ligands with selectivity and affinity to this GF and its receptors, aiming to understand their interactions and thus develop new strategies to tune their signaling capacity.

The regenerative potential of surfaces functionalized with TGF- β 1-binding peptide (Table 1) through azide-terminated SAMs and microcontact printing, and pre-loaded

1
2
3 with TGF- β 1, was evaluated by culturing human articular chondrocytes (hACs) on the
4 material (76). After 7 days of culture, more cells were observed on the peptide-
5 functionalized surfaces than on the bare azide SAMs. Chondrocytes cultured in the
6 absence of TGF- β 1 were found to be more extended, resembling the typical
7 morphology of fibroblasts, while those cultured in presence of TGF- β 1, exhibited a
8 round polygonal shape, representative of chondrocyte phenotype. In addition,
9 glycosaminoglycan (GAG) analysis revealed higher levels of GAGs in lysates of hACs
10 cultured on peptide-functionalized surfaces with bound TGF- β 1 compared to hACs
11 cultured on glass and with the GF free in the medium, and for cultures on peptide-
12 functionalized surfaces without TGF- β 1.
13
14
15
16

17 Using phage display, two peptides that bind specifically to the TGF- β receptor II (T β RII)
18 (Table 1) have been identified (66). These peptides can mimic or block distinct
19 functions of TGF- β I, and can be used to regulate these different functions, separately
20 or in concert, which are important for vascular therapy. The group of Kiessling also
21 used phage display to identify peptide ligands specific for TGF- β receptors I and II (65)
22 (Table 1). They showed that the identified peptides bind to the receptors on a region
23 different from the binding site used by TGF- β , thus not interfering with TGF- β signaling.
24 Therefore, these ligands can be applied as tool to examine the diverse cellular
25 functions of TGF- β , as well as to promote the identification of potential therapeutics.
26 Indeed, in later work, Kiessling and co-workers employed SAMs to present the
27 previously identified peptide sequences, which interact with both TGF- β receptors
28 (T β RI-ED and T β RII-ED), to provide localized and defined spatial signaling to cells (77).
29 As a proof of concept, they used NMuMG mouse mammary gland cells to investigate
30 the attachment of cells expressing TGF- β receptors to the surfaces displaying the T β R-
31 binding peptides. The cells bound to SAMs presenting either peptide (even at low
32 peptide densities, 4%), but not to the bare surfaces. They further demonstrated that
33 the functionalized surfaces activated Smad2/3 nuclear translocation (a hallmark of
34 TGF- β signaling).
35
36
37
38
39
40
41

42 These studies demonstrate the power of phage display to generate peptides that can
43 be used to regulate signaling pathways that lead to specific cell outcomes. Strategies
44 to control the beneficial roles of signaling pathways would be valuable for applications
45 in RM.
46
47

48 ***3D hydrogels for recreating specific (stem) cell or tissue environments***

49
50
51 Molecular design of biomaterials offers the opportunity to incorporate peptide ligands
52 that can be recognized by specific cell receptors or enzymes, and to control their
53 spatial and temporal availability for triggering regenerative events. The incorporation
54 of peptide sequences identified by phage display into molecularly-designed
55
56
57
58
59
60

1
2
3 biomaterials, and in particular, self-assembling peptide biomaterials, has been
4 reported by several groups.

5
6 Being the major inorganic constituent of bone and teeth, HAP has received great
7 attention as a target for phage display experiments. For example, the Sarikaya group
8 identified a HAP-binding peptide (Table 1) (44), which was then incorporated into a
9 peptide hydrogel capable of directing the mineralization of HAP (78) (Figure 3a). Other
10 studies describing peptides with preferential adsorption to HAP-based materials have
11 also been reported (45, 79, 80) (Table 1). Peptides with binding affinity to different
12 apatite substrates can be used to direct the growth of HAP on biomaterials surfaces
13 (81), or to improve the functional properties of HAP-based scaffolds, and thus enhance
14 bone regeneration.

15
16 The Stupp laboratory designed self-assembling peptides, known as peptide
17 amphiphiles (PAs), for RM applications. Of particular interest for the purpose of this
18 review, are PAs designed to bind GFs using peptide sequences derived by phage
19 display. They first reported a novel class of reverse PAs to enable the creation of
20 peptide assemblies with free N-terminal, which were not possible to obtain through
21 the original design. They were able to apply this new methodology to synthesize PAs
22 incorporating peptide sequences, derived via phage display and requiring a free N-
23 terminus, that bind GFs, BMP-2, and TGF- β (Table 1) (62), all involved in stem cell
24 differentiation. These PA molecules are known to form nanofibers by self-assembly
25 (Figure 3-b2), which at sufficiently high concentration, is accompanied by gelation
26 (Figure 3-b1). By permitting the direct binding of the GF to the PA nanofiber, gels
27 containing BMP-2 bound to PA allowed prolonged GF retention (Figure 3-b3). When in
28 solution, the BMP-2-bound PA nanofibers induced the differentiation of C2C12 pre-
29 myoblast cells into osteoblasts, as detected by an increased number of alkaline
30 phosphatase (ALP, marker for osteoblast differentiation)-positive cells (Figure 3-b4).

31
32 The BMHP motif was used by Gelain and co-workers (58, 82-86) to functionalize self-
33 assembling peptide scaffolds for culturing and controlling neural stem cell (NSC)
34 behavior for nervous tissue regeneration. In their pioneering work (83), they used
35 BMHP-functionalized self-assembling peptide hydrogel scaffolds for 3D culture of adult
36 mouse NSCs. In differentiation assays, the scaffolds containing BMPH motifs (BMHP1
37 and BMHP2, Figure 3-c3,c4) showed β -tubulin⁺ and nestin⁺ cells comparable with those
38 cultured on Matrigel (Figure 3-c1). β -Tubulin⁺ cells on BMPH scaffolds also showed
39 increased branching when compared with non-functionalized scaffolds (Figure 3-c2).
40 These results demonstrate the ability of these synthetic peptide nanofiber scaffolds to
41 be functionalized with different peptide motifs for the controlled 3D culture of diverse
42 cell types.

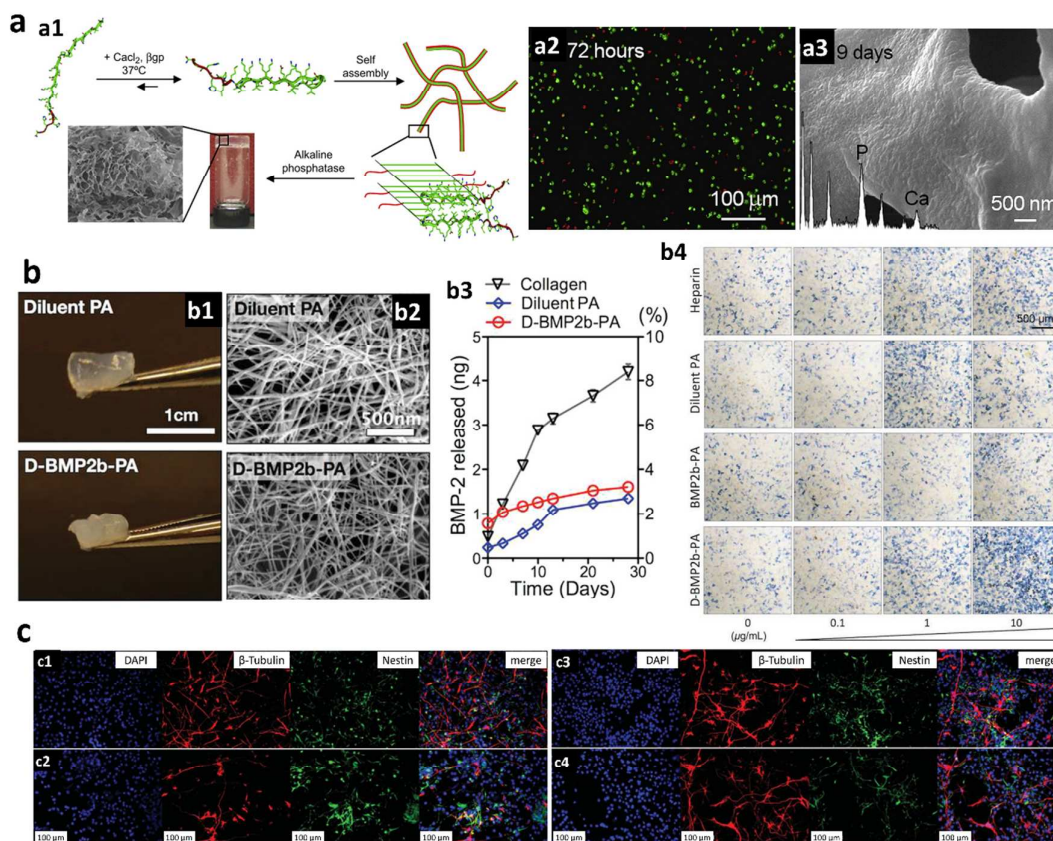


Figure 3. 3D biomaterials (hydrogels) functionalized with peptide sequences identified by phage display for *in-vitro* cell culture (proliferation and differentiation). **(a)** Self-assembled peptide hydrogels functionalized with HAP-binding peptides for periodontal regeneration; (a1) Schematic illustration of the peptide self-assembly and hydrogel formation; (a2) Fluorescence microscopy image of a live/dead assay on cementoblast cells encapsulated within self-assembling peptide gels showing viable cells; (a3) Scanning electron microscopy (SEM) image of the peptide gel showing the deposition of calcium-phosphate mineral by cementoblasts, as confirmed by the corresponding EDXS (inset). Reprinted and adapted from ref. (78). Copyright 2010 with permission from Elsevier. **(b)** BMP-2-binding PA (BMP2b-PA) nanofibers induced osteoblast differentiation of a myoblast cell line (C2C12) *in vitro*; (b1) Photographs of PA-based gels (D-BMP2b-PA: obtained by mixing equal ratios of BMP2b-PA with diluent PA at the same concentration); (b2) SEM micrographs of PA gels showing the network of filamentous nanostructures; (b3) *In vitro* release of BMP-2 from PA gels, with or without BMP-2-binding PA, in comparison to collagen sponges pre-loaded with BMP-2 up to 28 days; (b4) Optical micrographs of C2C12 cells stained for the detection of ALP on day 3 of culture in growth medium supplemented with treatment media containing $50\ \text{ng mL}^{-1}$ of BMP-2 with heparin or PAs at different concentrations. Adapted from (87). Copyright© 2014 Wiley-VCH Verlag GmbH & Co. KGaA, Weinheim. **(c)** NSC differentiation on 3D peptide nanofiber gel scaffolds functionalized with bone marrow binding peptides, BMHPs; (c1-c4) Inverted fluorescence microscopy images of differentiating adult mouse NSCs cultured *in vitro* during 7 days on: (c1) 1% Matrigel (positive control), (c2) non-functionalized RADA16 peptide gel (negative control), (c3) RADA16-BMHP1, and (c4) RADA16-BMHP2, stained for cell nuclei (blue), β -tubulin⁺ (red) for neurons, and nestin⁺ (green) for neural progenitors (green). Adapted with permission from ref. (83). Copyright 2006 PlosOne.

Chemically crosslinked hydrogels, such as those composed of poly(ethylene glycol) (PEG), have been functionalized with different peptide ligands to culture cells in 3D.

1
2
3 The Anseth group (88) functionalized PEG hydrogels with a basic fibroblast growth
4 factor (bFGF)-binding peptide, previously selected by phage display (63), to control GF
5 retention and sustained release for applications in GF-induced regeneration. To
6 enhance the affinity of the bound ligand for diffusible proteins (e.g. GFs) within the
7 hydrogel, they synthesized tri-functional peptides and examined how the molecular
8 structure of the affinity peptides affected their accessibility and binding using Forster
9 resonance energy transfer. They then showed that the optimal functionalization
10 strategy allowed the sustained release of bioactive bFGF able to induce the *in-vitro*
11 differentiation of the PC12 pheochromocytoma cell line. This affinity hydrogel could be
12 manipulated for GF retention, or delivery, and be easily applied in distinct RM
13 approaches, such as controlled stem cell differentiation *in-vitro*, or GF-mediated
14 wound healing *in-vivo*.
15
16
17
18
19
20

21 **Implantable biomaterials functionalized with peptide ligands identified by phage** 22 **display for promoting endogenous tissue repair *in-vivo*** 23

24
25 Tissue regeneration *in-vivo* can be enhanced by promoting the recruitment and
26 localization of stem cells into injured tissues and/or stimulating the function and
27 differentiation of local stem cells. This can be achieved by manipulating the properties
28 of the niche (e.g. promote angiogenesis or *de-novo* niches) or through the delivery of
29 active molecular regulators, directly or combined with a biomaterial, or by using
30 biomaterial sequestering GFs.
31
32
33

34 ***Stem cell homing*** 35

36 Using polycaprolactone (PCL, a FDA-approved polymer for medical applications)
37 electrospun meshes conjugated with phage-derived peptide (E7, Table 1) with affinity
38 for human bone marrow-derived MSCs (hBMSCs), Shao and co-workers showed
39 improved recruitment of MSCs *in-vivo* after implantation in full-thickness articular
40 osteochondral defects in a rat knee (51). Immunofluorescence staining of harvested
41 implants (Figure 4-a) showed that cells on the E7-conjugated PCL meshes were mostly
42 positive for CD44, CD90, and CD105 (MSCs surface markers), indicating that the
43 functionalized scaffold could selectively recruit and retain MSC-like cells from the bone
44 marrow. In contrast, cells in the PCL meshes conjugated with the cell adhesive peptide
45 RGD (with no cell specificity, control) showed lower levels of MSCs surface markers.
46 CD68 staining was also used to assess the inflammatory response. Results from
47 immunofluorescence staining showed that there was a high proportion of
48 inflammatory cells in the RGD-conjugated PCL meshes, while CD68⁺ cells were scarce in
49 the E7-conjugated scaffold, suggesting only a minor inflammatory response. For the
50 bare PCL meshes, only few cells could be detected into the mesh, due to the
51 unfavorable cell adhesion properties of PCL. The E7 peptide could be further applied
52
53
54
55
56
57
58
59
60

1
2
3 for functionalizing other biomaterials for effective MSC-homing in stem cell-based
4 tissue repair strategies.
5

6
7 ***Controlled release of growth factors (GFs)***

8 TGF- β 1 is known to play a critical role in the development, growth, maintenance and
9 repair of articular cartilage. To this end, the Stupp group designed self-assembled
10 peptide nanofibers for cartilage regeneration, using a peptide sequence derived by
11 phage display with binding affinity for TGF- β 1 (Table 1) (89). When implanted into a
12 full-thickness chondral defect in a rabbit model (Figure 4-b1), these self-assembled gels
13 were shown to support the regeneration of articular cartilage (Figure 4-b2, b3) with or
14 without the supplementation of TGF- β 1, as detected by formation of hyaline-like tissue
15 (GAGs and collagen II staining, Figure 4-b3) within the defect space.
16
17

18
19 To promote bone healing, Hamilton *et al.* (17) developed a novel strategy to deliver
20 osteogenic GFs, such as BMP-2, in a collagen biomaterial carrier. This carrier contained
21 a bifunctional peptide (BC-1) that displayed BMP-2 and collagen-binding domains, both
22 identified by phage display (Table 1). This strategy allowed the simultaneous binding of
23 GFs directly to an implantable biomaterial, without the requirement for any
24 conjugation steps, thus allowing the controlled delivery of GFs at the implantation site.
25 To test the ability of this system to promote bone formation *in-vivo*, the authors
26 injected BMP-2 within a collagen gel, containing or lacking BC-1, into the subcutaneous
27 regions of Sprague Dawley rats (rat ectopic bone formation model). Histological
28 analysis and evaluation of the explants showed significantly higher osteogenic cellular
29 activity, bone area formed, and bone maturity in the presence of BC-1 (Figure 4-c1,
30 c2).
31
32
33
34
35
36
37
38
39
40
41
42
43
44
45
46
47
48
49
50
51
52
53
54
55
56
57
58
59
60

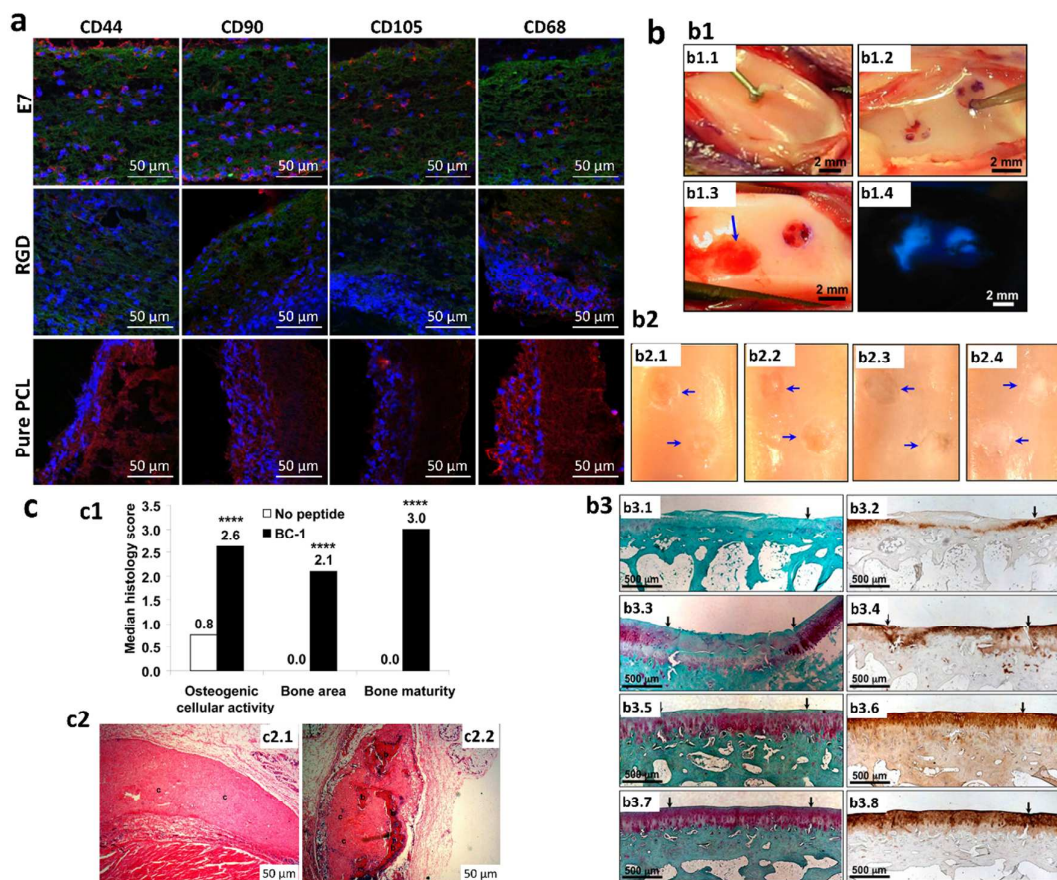


Figure 4. The application of phage-derived peptides for *in-vivo* tissue regeneration. (a) *In-vivo* stem cell homing by PCL electrospun meshes functionalized with E7 peptide with specific affinity for MSCs; (a1) Confocal microscopy images of peptide-conjugated PCL electrospun meshes harvested 7 days after implantation in full-thickness articular osteochondral defects in rats and stained by immunofluorescence for specific MSC (CD44, CD90, CD105) and inflammatory (CD68) markers (green: FITC, blue: Hoeschst33258, red: CD44/CD90/CD105/CD68 counterstained with Cy3 & Cy5). Reprinted and adapted from ref. (51). Copyright 2012 with permission from Elsevier. **(b)** PA molecules displaying binding epitopes for TGF β -1 support the regeneration of full thickness chondral defects in articular cartilage; (b1) Surgical and implantation procedure showing: (b1.1) full thickness articular cartilage defects made with a microcurette in rabbit trochlea; (b1.2) Microfracture holes through the subchondral bone using a microawl to promote bleeding into the defect; (b1.3) Injected PA gel in the defect (arrow); (b1.4) PA gel labeled with a fluorescent dye contained within the cartilage defects after injection. (b2) Images of articular cartilage defects after 12 weeks of implantation with: (b2.1) 100 ng/mL TGF- β 1; (b2.2) Filler PA + 100TGF; (b2.3) 10%TGFBP + 100TGF, (b2.4) 10%TGFBP alone. (b3) Microscopy images of tissue sections of articular cartilage defects obtained from histological and immunohistochemical analysis and stained for GAGs using safranin-O (left panel) and type II collagen (right panel) 12 weeks after treatment with: (b3.1, b3.2) 100 ng/mL TGF- β 1; (b3.3, b3.4) filler PA + 100TGF; (b3.5, b3.6) 10%TGFBP + 100TGF; (b3.7, b3.8) 10%TGFBP alone. Reprinted with permission from (89). Copyright (2010) Proceedings of the National Academy of Sciences of the United States of America. **(c)** An injectable collagen gel containing a bifunctional peptide (BC-1) with affinity for collagen and BMP-2 enhances retention of BMP-2 and increases ectopic bone formation; (c1) Osteogenic cellular activity, bone area and bone maturity scored from H&E slides (c2) and by two observers; (c2) Histology images (H&E staining) from the rat ectopic model; (c2.1) 2 μ g BMP-2 in 1.5% collagen gel; (c2.2) 2 μ g BMP-2 with 50-fold molar

1
2
3 excess of BC-1 in 1.5% collagen gel. (b – bone zones; c – collagen zones; cells are stained blue). Adapted
4 with permission from ref. (17). Copyright 2010 PlosOne.

5
6 Degenerative joint diseases, such as osteoarthritis (OA), are characterized by
7 progressive cartilage matrix degradation. Targeted therapies for damaged articular
8 cartilage can offer the opportunity for localization of bioactive proteins, such as GFs,
9 that can enhance the synthesis of a more hyaline-type cartilage. Towards this
10 challenge, Hubbell's group described the synthesis and functionalization of
11 nanoparticles for the release and retention of drugs inside articular cartilage through
12 the identification of a peptide specific for the principal component of the cartilage
13 matrix (collagen II α 1, Table 1) (40). After intra-articular injection in a mouse model,
14 conjugation of the peptide to nanoparticles led to higher retention of the
15 nanoparticles within the ECM of articular cartilage (72-fold increase after 48 h) when
16 compared to nanoparticles functionalized with a non-targeted (control) peptide. Such
17 an approach could be used to deliver and localize specific GFs for cartilage repair.
18
19
20
21
22
23
24

25 **Nanobiomaterial carriers functionalized with peptide ligands identified by phage** 26 **display for genetic manipulation of cells *in-vitro* and *in-vivo*** 27

28 The field of gene therapy for tissue repair and regeneration would benefit considerably
29 from the isolation of peptides that can target endocytosing receptors on specific cells
30 (90). Internalization of gene delivery systems is a prerequisite for efficient transgene
31 expression. Peptides that can be internalized by cells are likely to be useful for
32 nonviral-mediated gene delivery, where some current systems do not have the ability
33 to enter the cells (e.g. polycation-DNA complexes). Gene therapy vectors could be
34 modified with specific peptide ligands and delivered intravenously to transfect only
35 specific cells, thus improving their efficacy and reducing the toxicity of the process.
36 Therefore, many research groups have attempted to select cell-binding and cell-
37 penetrating peptides ("homing peptides") using phage display for targeting specific cell
38 types (91, 92).
39
40
41
42
43

44 **Targeted gene therapy** 45

46 The use of phage display to identify cell-selective and cell-entry peptides as gene
47 therapy vectors was first reported by Barry and colleagues in 1996 (92). They displayed
48 12- and 20-mer peptide libraries on pIII protein of fdTET phage and, by screening the
49 libraries on mammalian cells, isolated cell-binding peptides. This was the first
50 demonstration that cell-selective peptides could be identified by panning peptide
51 phage libraries on cells, without prior information of the target receptors. However, in
52 this pioneering work, they did not demonstrate the delivery of functional genes to the
53 nucleus of specific mammalian cells.
54
55
56
57
58
59
60

1
2
3 In attempt to develop *in-situ* gene therapy, Schmidt *et al.* (57) identified peptide
4 ligands (Table 1) that selectively bound to mouse NPCs from phage display peptide
5 libraries. They subsequently conjugated the identified peptides to wild-type capsid and
6 capsid-mutated adenovirus (Ad) vectors and tested their targeting potential *in-vitro*
7 and *in-vivo*, respectively. Peptides were shown to mediate Ad binding and infection of
8 NPCs *in-vitro*, and selective transduction of NPCs in the brain of adult C57BL/6 mice, as
9 shown by the presence of nestin (Figure 5-a1), a NPC-specific marker, co-localized with
10 green fluorescent protein (GFP) (Figure 5-a2). Injection of a non-specific peptide failed
11 to transduce cells in the dentate gyrus, as seen by the absence of GFP expression
12 (Figure 5-a3), while injection of wild-type capsid AdGFP resulted in transduction of
13 non-NPCs, such as astrocytes and neurons (Figure 5-a4).
14
15
16
17

18 Using a non-viral vector (poly(amido)amine (PAMAM) dendrimers) functionalized with
19 bone-targeting peptides, identified by phage display and having high (HAB) and low
20 (LAB) affinity binding to mouse MSCs, Santos and co-workers (93) were able to
21 promote the uptake of plasmid DNA (pDNA) by rat MSCs (rMSCs). HAB peptide-
22 functionalized dendrimers led to increased accumulation of pDNA inside cells (Figure
23 5-b1). In addition, the presence of HAB bone-targeting peptides on the dendrimer
24 surface led to higher transfection levels than those obtained with native dendrimers,
25 measured by luciferase (Luc) gene expression (Figure 5-b2). Similarly, Ma and
26 colleagues (53) used a rMSC-homing peptide, identified by phage display (Table 1), to
27 improve the targeting capability of protamine/DNA lipoplex (LPD) liposomes to rMSCs
28 for the delivery of Sleeping Beauty (SB) transposon plasmid. They also incorporated
29 the positively charged nuclear localization signal (NLS) peptide to promote
30 translocation of gene materials into the nucleus. By combining rMSC-targeting ability
31 and NLS peptide into LPD liposomes, the transfection efficiency was improved, in
32 comparison to control peptides (randomly selected), by enhancing the receptor-
33 mediated endocytosis of LPD liposomes and their accumulation in the nucleus. They
34 showed that the SB transposon and targeting LPD system did not result in cell toxicity,
35 and did not promote osteogenic differentiation, suggesting the potential of this system
36 for effective nonviral gene delivery in stem cell therapy.
37
38
39
40
41
42
43
44

45 By panning on porcine skin, Hsu and Mitragotri (60) identified a peptide by phage
46 display, named as skin permeating and cell entering (SPACE) peptide, to enable the
47 diffusion of macromolecules across the stratum corneum into the epidermis and
48 dermis. The peptide also showed ability to translocate the membrane of skin cells,
49 such as keratinocytes, fibroblasts, and endothelial cells (Figure 5-c1). The efficacy of
50 the peptide to carry and release small interfering RNA (siRNA) for GFP (Figure 5-c2.1)
51 and IL-10 was tested *in-vitro* and *in-vivo* (Figure 5-c2.2), respectively. Peptide
52 conjugation with siRNA led to enhanced cell penetration and absorption into the skin,
53 and knockdown of corresponding protein targets. On the contrary, however, no
54
55
56
57
58
59
60

substantial knockdown was obtained with only siRNA or SPACE or using control siRNA conjugated with SPACE or a control peptide.

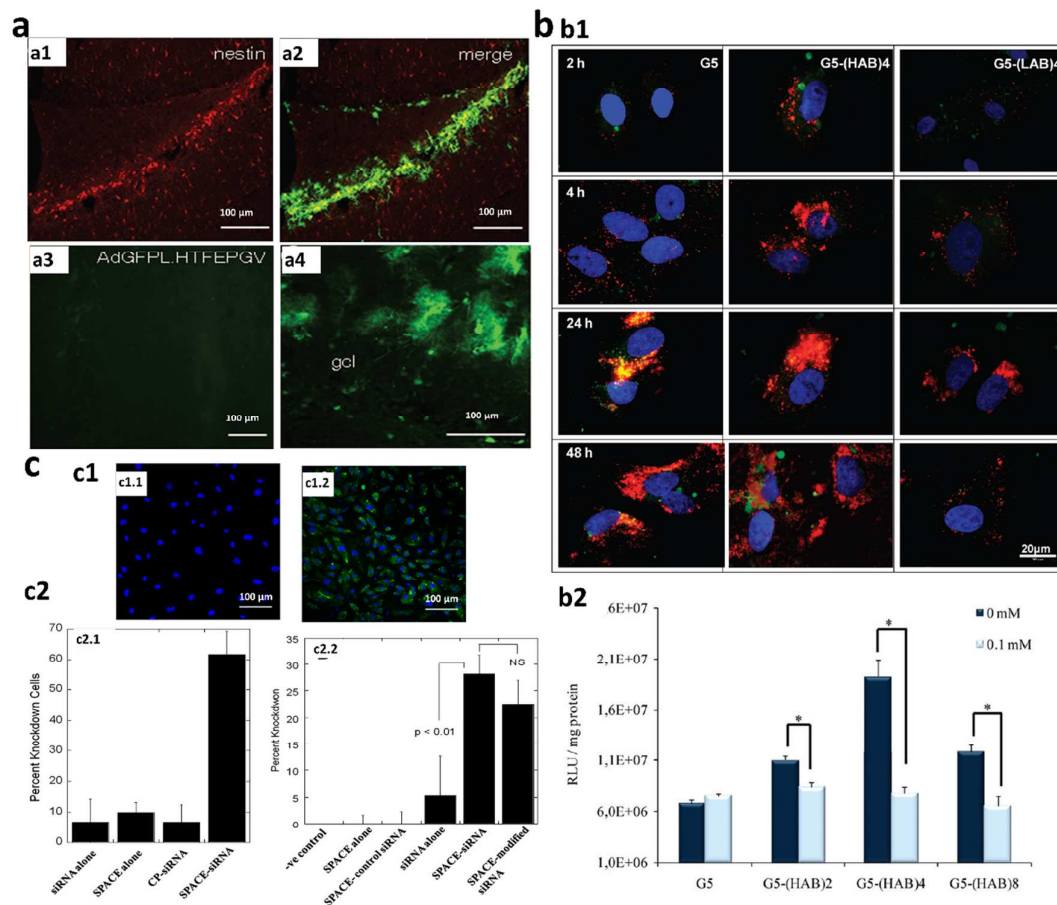


Figure 5. Cell-targeting gene delivery for selective and more efficient *in-vitro* and *in-vivo* gene therapy. (a) Selective transduction of NPCs in adult C57BL/6 mouse brain by capsid-mutated AdGFPL.VPTQSSG vector. Fluorescence-activated laser scanning microscopy images of brain sections analyzed by immunohistochemistry after injection of: (a1, a2) PEGylated AdGFPL.VPTQSSG, (a3) AdGFPL.HTFEPGV, (a4) AdGFP into the dentate gyrus of adult mice. Nestin (red fluorescence, a1) and merge (yellow a2); Abbreviations: AdGFP, adenoviral vector that expresses GFP; AdGFPL, adenoviral vector that expresses GFP-Luc; VPTQSSG, NPC-specific binding peptide; HTFEPGV, unspecific peptide; gcl, granular cell layer;. Reprinted and adapted from ref. (57). Copyright 2007 with permission from John Wiley and Sons. (b) Targeted gene delivery using PAMAM dendrimers functionalized with MSCs binding peptides; (b1) Fluorescence microscopy images showing intracellular localization of (RITC)-labeled pDNA (red) in MSCs transfected with native dendrimers (unconjugated, G5) and dendrimers conjugated with 4 peptide arms [G5-(HAB)4, G5-(LAB)4] as vectors. The endosomal-lysosomal system was stained with LysoSensor Green DND-189 (green), and the nucleus with DAPI (blue); (b2) Luc gene expression obtained with dendrimers (native and conjugated with 2, 4 and 8 HAB peptide arms) with and without pre-saturation of cell receptors by HAB peptide (0.1 mM). Reprinted with permission from (93). Copyright (2010) American Chemical Society. (c) Delivery of siRNA into the skin and cells using SPACE peptide; (c1) Confocal microscopy images of human umbilical vein endothelial cells (HUVECs) (nuclei stained in blue) treated with: (c1.1) PBS (control), (c1.2) FITC-labeled SPACE peptide for 24 h; (c2) Delivery of siRNA *in vitro* and *in vivo*; (c2.1) Percentage of knockdown of GFP in GFP-expressing endothelial cells; (c2.2) Percentage of

1
2
3 knockdown of interleukin-10 (IL-10) in mice after 24 h of treatment. Reprinted with permission from
4 (60). Copyright (2011) Proceedings of the National Academy of Sciences of the United States of America.

5
6 Using a cartilage affinity peptide (CAP, Table 1) conjugated with polyethyleneimine
7 (PEI) for DNA complexation (CAP-PEI/DNA) in *in-vivo* cartilage-targeted gene delivery,
8 Pi *et al.* (48) showed that the CAP-functionalized vector led to a nine-fold higher
9 transfection efficiency in cartilage than the scrambled peptide-conjugated vector.
10 However, no statistical difference in the transfection efficiency was observed in the
11 synovium between the vectors modified with targeted (CAP) and control (scrambled)
12 peptide.
13

14
15 The identification of peptide ligands binding to receptors in organelles of mammalian
16 cells (Table 1) was recently reported (61). When chemically fused to penetratin, the
17 identified peptide was internalized and localized in the mitochondria, promoting cell
18 death. This study demonstrated the further utility of phage display for subcellular
19 targeted drug delivery. Advances in targeted intracellular delivery selectivity also has
20 implications for RM, namely, in RNA interference (RNAi)-based anabolic therapies,
21 such as the delivery of osteogenic siRNAs specifically to osteoblasts (bone cells), aimed
22 at promoting bone formation (94, 95).
23
24
25
26

27 **Imaging probes functionalized with peptide ligands identified by phage display for** 28 **targeted imaging of cells and tissues *in-vitro* and *in-vivo***

29
30 Clinical imaging is an essential tool in RM. First, it is important to characterize the
31 status of the damaged/diseased tissue for pre-treatment planning, and second, it is
32 necessary to evaluate the risks and efficacy of the therapy (post-transplant
33 assessment) (96).
34
35

36 ***Injured and regenerating host environment***

37
38 The environment in injured or diseased tissues is not favorable for transplanted cells.
39 Some tissues produce scars (e.g. fibrotic scar, glial scar) after injury, and this scarring
40 process prevents engraftment of stem cells with the neighboring tissues. Additional
41 factors that contribute for a hostile condition in damaged tissues include the presence
42 of inflammatory cytokines and limited oxygen and nutrient delivery. Aging of the stem
43 cell niche and corresponding alteration of the acellular components can cause loss of
44 stem cell functionality. Thus, imaging of the niche properties, including tissue
45 architecture (structural integrity/morphological alterations), and molecular and
46 cellular composition (e.g. ECM, GFs, cell populations), could be beneficial for ensuring
47 that cells are hosted in a healthy environment (non-necrotic tissues). Peptides can be
48 combined with fluorophores or radioisotopes for the development of new probes (97),
49 as they provide numerous benefits over antibodies; they have higher stability and
50 lower immunogenicity, diffuse faster (owing to their small size allowing better tissue
51 penetration), and are easier to synthesize.
52
53
54
55
56
57
58
59
60

1
2
3 Peptide sequences binding to major components of the ECM of tissues, such as
4 collagen and HA (Table 1), have been identified by phage display. These sequences
5 have been further developed into molecular probes to detect these macromolecules in
6 different tissues (e.g. pericardium, skin).
7

8 HA plays a central role in the wound healing process, and influences stem cell behavior
9 (98, 99). The HA-binding peptide, described as Pep-1 in the literature, has been
10 biotinylated for identification of HA in the skin (42).
11

12 To improve the affinity of a phage-derived collagen-binding peptide for detecting
13 collagen I in tissues, and to improve contrast/detection, the Meijer group proposed a
14 new approach to display phage-derived peptides on dendritic architectures (18, 38). In
15 this system, a dendron mimics the pentavalent head of the phage (Figure 6-a1). The
16 system was then tested using a collagen-specific 7-mer peptide against collagen type I
17 from rat tails (38). Pentavalent display of collagen-binding peptides on dendrimer
18 wedges enhanced affinity for collagen by 100-fold when compared with the
19 monovalent peptide (38), allowing selective staining of collagen in tissues containing
20 collagen arranged in different levels of organization (fibrils, fibers, fiber bundles). Using
21 0.6 μM fluorescein-labeled pentameric peptide on pig parietal pericardium, a highly
22 defined fibrous network with fibers of 2 μm in thickness was observed (Figure 6-a2).
23 This result demonstrate that the identified peptide, derived from rat collagen, also
24 binds to collagen of different species. The monovalent form of the collagen binding
25 peptide at the same concentration (Figure 6-a3) did not allow collagen detection.
26 Comparable collagen fibrillar structures were visualized as for the pentameric peptide
27 when using 60 μM of the monovalent peptide, but the intensity of background
28 fluorescence was higher (Figure 6-a4). A naturally occurring collagen binding protein
29 (CNA35) was used as a comparison with the fluorescein-labeled pentavalent peptide.
30 Both probes allowed visualization of collagen fibers with the same orientation, but the
31 pentameric peptide led to a more specific stain when compared to CNA35 (Figure 6-
32 a5-a7).
33
34
35
36
37
38
39
40

41 Optical and nuclear imaging agents could be coupled to ECM-binding peptides to allow
42 clinical imaging and characterize organ/tissue morphology (e.g. degraded matrix)
43 before and after the therapies (matrix formation as a result of regeneration).
44

45 Lee and collaborators reported the results of panning against stabilin-2 (64) (Table 1),
46 known to be produced by activated macrophages and also strongly expressed in
47 smooth muscle cells and endothelial cells of atherosclerotic lesions. The identified
48 peptide sequence was found to bind specifically to stabilin-2 and localize to
49 atherosclerotic plaques *in-vivo*. In addition, the peptide was conjugated with
50 fluorescently tagged glycol chitosan nanoparticles and administered to apolipoprotein
51 E-deficient mice through direct injection into the left ventricles. The peptide-
52 conjugated nanoparticles were found to accumulate in the atherosclerotic lesions,
53 while control nanoparticles were not visible. These studies revealed peptide ligands
54 that can be used for selective molecular imaging of atherosclerosis.
55
56
57
58
59
60

1
2
3 Phage display-derived vascular adhesion molecule 1 (VCAM-1)-specific peptide has
4 allowed targeted imaging of activated endothelium under inflammatory conditions by
5 fluorescence imaging and magnetic resonance imaging (MRI, Figure 6b), and has
6 enabled the visualization of structural abnormalities in the aortic wall (67). Similar
7 probes could be developed against pro-inflammatory cytokines implicated in tissue
8 injury (e.g. tumor necrosis factor α (TNF- α); interleukin 1- β (IL-1 β)) to characterize
9 tissue functionality and delineate the feasibility of the cell therapy.
10

11
12
13 Phage-derived peptides would be also useful to measure regeneration outcomes, such
14 as angiogenesis and formation of new tissue. For example, angiogenic vasculature has
15 been assessed by imaging the binding of RGD-containing peptides conjugated to PET
16 imaging agents to specific integrins on the cell surface (100). Using the above-
17 described probes, the production and structure of tissue-specific ECM components
18 (e.g. collagen II in cartilage or HAP in bone or tooth) could be visualized independently
19 and non-invasively through different imaging modes. Similarly, the functionality of
20 newly-formed tissue could be detected by assessing the presence of specific cell
21 populations using ligands for phenotype-specific markers. The discovery of novel
22 peptide ligands for the development of molecular imaging probes with enhanced
23 specificity for detecting constant changes in the environment of damaged and
24 regenerating tissues would greatly benefit cell-based therapies.
25
26
27
28
29
30
31

32 **Cell labeling/tracking**

33
34 Tracking the distribution, function, and fate of transplanted cells using noninvasive
35 imaging is an important goal in RM. The ability to assess cell localization, viability,
36 growth, differentiation, and engraftment in the host would be extremely valuable.
37 However, cells administered into humans cannot be tracked unless they are first
38 labeled *in-vitro*. Cells can be labeled directly, using chemical agents, or indirectly, by
39 inclusion of reporter genes. Cell labeling methods should be specific, nontoxic, and
40 stable (i.e. label agents should remain in the target cells for suitable periods of time to
41 allow correlation with cell numbers).
42
43
44

45 Several cell-binding peptides have been identified, with the isolation of stem-cell
46 binding peptides being of particular utility for RM applications (100) (Table 1). These
47 peptides can be exploited for cell labeling/imaging and isolation purposes. For
48 example, Ma's group (54-56, 59) used phage-derived cell-binding peptides conjugated
49 with quantum dots (QDs, light emitting agents) to specifically label ESCs. By panning on
50 rhesus macaque ESCs, they identified the sequence, APWHLSSQYSRT (Table 1), with
51 high affinity for undifferentiated ESCs. They subsequently conjugated the peptide to
52 CdSe-ZnS QDs (Figure 6-c1) and showed that the conjugates could bind efficiently and
53 selectively to ESCs, with no binding observed for other cell types (primary mouse
54 embryonic fibroblast, PMEF, Figure 6-c3) and ESCs from other species (mouse ESCs,
55
56
57
58
59
60

1
2
3 Figure 6-c5), or when control QDs were used (Figure 6-c4, c6). The E7 peptide (Table
4 1), known to bind hMSCs, was conjugated to gadolinium(Gd)-1,4,7,10-
5 tetraazacyclododecane-1,4,7,10-tetraacetic acid (DOTA) for labeling MSCs for MRI
6 (101). *In-vitro* studies showed Gd-DOTA-E7 yielded minimum labeling efficacy, but
7 good contrast enhancement.
8
9

10 Identification of peptides that interact with stage-specific cellular targets (e.g.,
11 differentiation stage) would be useful for assessing molecular profiles of cells *in-vivo*
12 (e.g., imaging differentiation of transplanted cells). Zhao *et al.* (59) identified a peptide
13 with the ability to bind NSCs derived from rhesus monkey ESCs, and used this peptide
14 combined with QDs for cell imaging. This study described for the first time the use of
15 phage-derived peptides for studying ESC differentiation by optical imaging.
16
17
18

19 A problem with these imaging agents is that the signal cannot be used to distinguish
20 live from dead cells, and is not certain whether or not these probes will be retained by
21 cells in the long term. Previous studies indicated that after cell death, contrast agents
22 can be passed to host cells, producing false positives (102, 103). Thus, monitoring stem
23 cell fate may require a combination of complementary imaging methods, such as
24 fluorescence and magnetic resonance, to allow the correlation between anatomical
25 localization of labeled stem cells and cell viability. Reporter genes represent a potential
26 solution to this issue, although this can pose additional safety and regulatory
27 problems. Phage display could also contribute towards the development of molecular
28 probes that would bind only viable cells resulting in the release of the label after cell
29 death. Since dead cells have a compromised cell membrane, it might be possible to
30 identify a specific ligand for live cells by panning on dead cells first (pre-clearing).
31
32
33
34
35
36
37
38
39
40
41
42
43
44
45
46
47
48
49
50
51
52
53
54
55
56
57
58
59
60

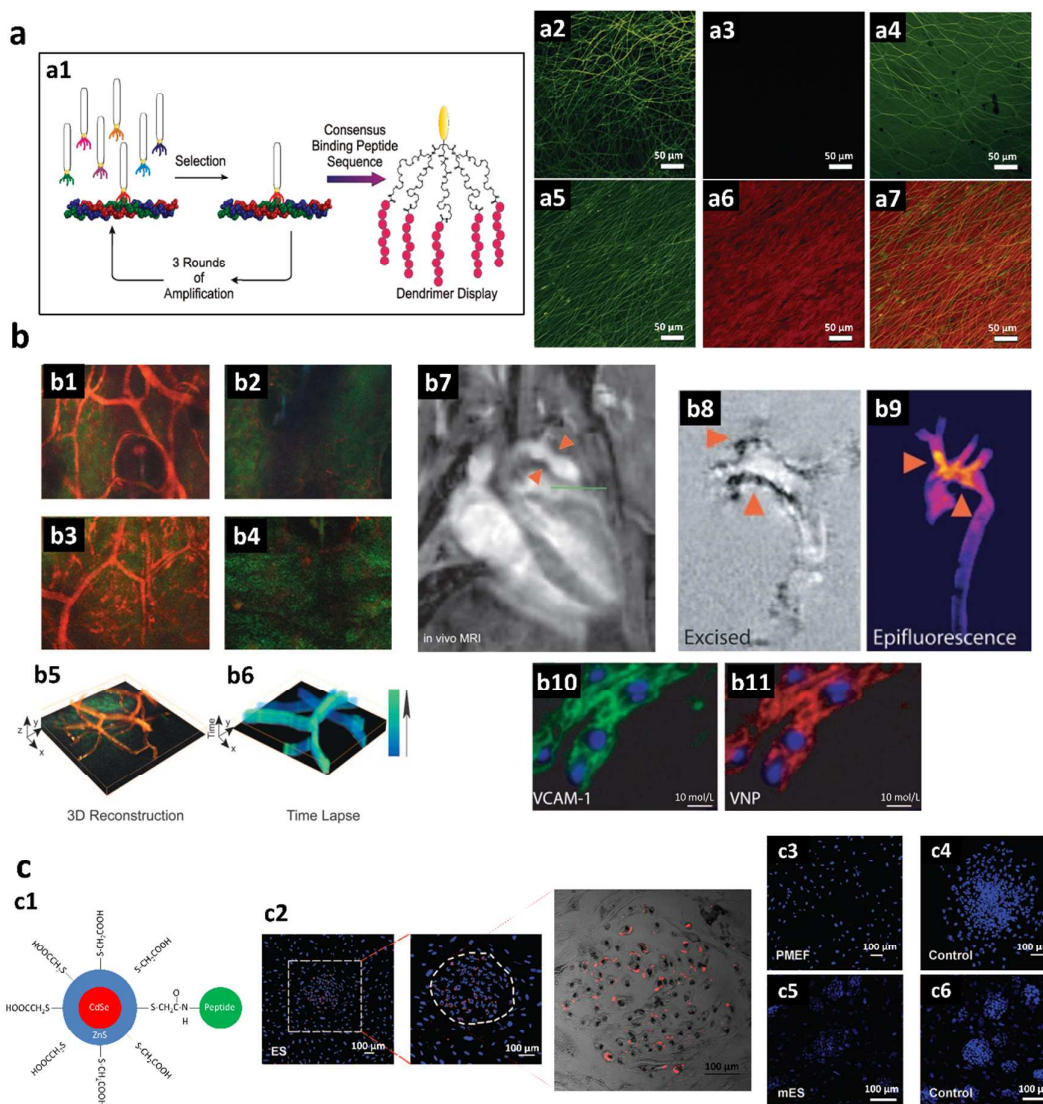


Figure 6. The application of phage-derived peptides for targeted imaging of cells and tissues *in-vitro* and *in-vivo*. (a) Collagen I-specific probe based on collagen-binding peptide displayed on dendrimer edges; (a1) Collagen-binding peptide displayed on dendrimer edges resembling the typical pentavalent structure of phages. Laser scanning confocal microscopy images of pig parietal pericardium incubated with: (a2) 0.6 μM fluorescein-labeled peptide pentamer; (a3, a4) fluorescein-labeled monovalent collagen binding peptide at 0.6 μM and 60 μM ; (a5-a7) 6 μM AlexaFluor568-labeled CNA35 (red) followed by 0.6 μM fluorescein-labeled peptide pentamer (green) (co-staining). Adapted with permission from ref. (38). Copyright 2009 American Chemical Society. (b) Detection of VCAM-1 by MRI and fluorescence imaging using VCAM-1-binding peptide (VP) and multimodal nanoparticles (VNPs) in atherosclerotic lesions. Intravital confocal microscopy images of mouse ear with (b1, b3) or without (b2, b4) mTNF- α -induced inflammation at 4 (b1, b2) and 24 h (b3, b4) after intravenous injection of VNP (red). Green color in the images is due to the tissue autofluorescence; Images obtained from the 3D stack reconstruction of the Z series (b5) from (b3) and of the time series (b6) of VNP staining within the vessels (each time point is shown as an individual slice in the Z direction and the level of peptide staining (low to high) is given by the color scheme (blue to green)). *In-vivo* (b7) and *ex-vivo* (b8) MRI of the aorta of cholesterol-fed apoE^{-/-} mice using gadolinium-protected graft copolymer (Gd-PGC) shows defined vascular lumen and aortic abnormalities such as narrowing (b7, arrows) and low signal changes caused

1
2
3 by VNP localization (arrows, b8); (b9) Epifluorescence image of excised aorta using fluorescent labeled
4 peptide confirming details observed in (b8); (b10, b11) Immunofluorescence images of aorta sections
5 revealing co-localization of VCAM-1 (green) and VNP (red). Nuclei in b10 and b11 are stained with DAPI
6 (blue). Bars = 10 μm . Adapted with permission from Lippincott Williams and Wilkins/Wolters Kluwer
7 Health: Circulation Research (67), copyright 2005. (c) Targeted imaging of ESCs using peptide-conjugated
8 QDs. (c1) Schematic of CdSe-ZnS QDs conjugated with APWHLSSQYSRT peptide (green sphere); (c2)
9 Fluorescence and bright-field microscopy images of ESCs (cell nuclei in blue, Hoechst 33258) after
10 incubation with peptide-QDs (red) showing their binding to ESC colonies (inside dashed line); (c3)
11 Fluorescence microscopy image of peptide-QDs with PMEF cells which are used as a feeder layer
12 (outside dashed line); (c4, c6) Fluorescence microscopy images of cells with free QDs (without
13 conjugated peptides, control); (c5) Fluorescence microscopy images mESCs peptide-conjugated QDs;
14 Adapted with permission from ref. (56). Copyright 2010 PlosOne.
15
16
17

18 **CONCLUDING REMARKS AND OUTLOOK**

19
20 The ability to display a large and highly diverse collection of random peptide sequences
21 on the coat-proteins of phages offers the possibility to discover new interactions with
22 useful targets, often without knowing their structure. The field of phage display
23 technology has evolved significantly from when it was first developed for mapping
24 interactions between proteins, and has expanded into other areas that benefit from
25 the discovery of new interacting ligands. This review demonstrates the usefulness of
26 phage display in the emerging field of RM, suggesting opportunities for further
27 applications. However, we must consider the challenges associated with phage-derived
28 peptides before their translation into useful RM tools. When used as linear monomers,
29 isolated peptide ligands usually show poor affinity for their targets, as this
30 presentation differs significantly from the original display (valency and orientation) on
31 the phage particles. Multimerization (conjugation of multiple peptide copies to a
32 surface of a nanoparticle, like dendrimers, liposomes, or micelles) has been proven to
33 increase affinity of the ligand for its targets, but the affinity of these multivalent
34 peptide platforms also depends on the density of receptors on the cell periphery. In
35 addition, when displayed on the phage, peptides are fused to the coat protein through
36 the C-terminus and have a free N-terminus. This feature is not always taking into
37 account when presenting phage-derived peptides into multivalent carriers. This
38 stresses the importance of the use of biomaterials engineering to enable the peptides
39 to be displayed in the precise and optimal multimeric conformation for interaction
40 with cell receptors. Presenting peptides within a biomaterials platform also provides
41 protection against proteolytic degradation, which is essential for prolonging their half-
42 life *in-vivo*.
43
44
45
46
47
48
49
50
51

52 It should be noted that many of the sequences described in this review were obtained
53 from targets derived from multiple species. Thus, it is necessary to confirm if these
54 peptides also bind to the same targets in humans. Although cell-binding peptides can
55 be used without knowing their specific receptors, identification of their cellular targets
56 is essential for gaining clinical approval, as emphasized by Gray and Brown (100). It is
57
58
59
60

1
2
3 also useful for obtaining information about the heterogeneity of the protein repertoire
4 on the cell surface and how it varies among cell types and states.
5

6 To accelerate the safe application of phage-derived peptides within the field of RM,
7 the next logical steps will be their further optimization and validation *in-vitro* and *in-*
8 *vivo*, in terms of affinity, specificity, activity, stability, and biodistribution.
9

10 While binding has been the basis for peptide screening in phage display, selection
11 based on function might be useful for certain RM approaches (e.g. controlled stem cell
12 differentiation). In a recent perspective article (104), Lerner highlighted the potential
13 of intracellular combinatorial (unbiased) antibody libraries as a discovery tool to select
14 antibodies able to bind unknown receptors or to identify new roles of common
15 receptors. They showed that infection of BMSCs with unbiased libraries led to the
16 selection of various antibody agonists that induced proliferation of cells, or
17 proliferation followed by differentiation or trans-differentiation into neural cells,
18 indicating new roles for identified receptors in differentiation. These studies suggest
19 new ways to regulate cell fates by selecting cell-binding antibodies or peptides on the
20 basis of function (e.g., ability to activate a given receptor involved in inducing
21 differentiation).
22
23
24
25
26

27 With further advances in biology and RM, there are enormous opportunities for phage
28 display to contribute tools for research and applications in such fields. Led by a vibrant
29 research community in biology and RM, phage display technology will have a broad
30 range of applications in the future.
31
32

33 34 35 **ACKNOWLEDGMENTS**

36 This work was supported by national funds through the Portuguese Foundation for
37 Science and Technology under the scope of the project PTDC/EBB-BIO/114523/2009
38 and by the European Regional Development Fund (ERDF) through the Operational
39 Competitiveness Programme "COMPETE" (FCOMP-01-0124-FEDER-014758). The
40 authors also thank the financial support of the Portuguese Foundation for Science and
41 Technology under the strategic funding of UID/BIO/04469/2013 unit and RECI/BBB-
42 EBI/0179/2012 (FCOMP-01-0124-FEDER-027462) and the European Union under the
43 Marie Curie Career Integration Grant SuprHApolymers (PCIG14-GA-2013-631871).
44
45

46 We thank L. Kluskens, from the Center of Biological Engineering at the University of
47 Minho (Portugal) for his expert opinion on phage display and valuable comments
48 during the reading of the manuscript. We are also very grateful to A. Mata from the
49 School of Engineering & Materials Science at Queen Mary University of London for his
50 insightful comments and suggestions on the manuscript.
51
52
53
54
55

56 57 58 59 60 **ABBREVIATIONS**

1
2
3 **Ad:** adenovirus; **ALP:** alkaline phosphatase; **ASCs:** adipose stromal cells; **ATs:** alkanethiols; **BC-**
4 **1:** bifunctional peptide 1; **BRASIL:** biopanning and rapid analysis of selective interactive
5 ligands; **bFGF:** basic fibroblast growth factor; **BMHP:** bone marrow homing peptide; **BMP-2:**
6 bone morphogenetic protein 2; **BMSCs:** bone marrow stem cells; **C3:** complement 3; **CAP:**
7 chondrocyte-affinity peptide; **cBMHP:** cyclic BMHP; **cdDNA:** complementary DNA; **Col:** collagen;
8 **DMEM:** Dulbecco's modified eagle medium; **DNA:** deoxyribonucleic acid; **DOTA:** 1,4,7,10-
9 tetraazacyclododecane-1,4,7,10-tetraacetic acid; **ds:** double stranded; **EC₅₀:** half maximal
10 effective concentration; **ECM:** extracellular matrix; **ELISA:** enzyme-linked immunosorbent
11 assay; **ESCs:** embryonic stem cells; **FDA:** US Food and Drug Administration; **FITC:** Fluorescein
12 isothiocyanate; **GAG:** glycosaminoglycan; **Gd-PGC:** gadolinium-protected graft copolymer; **GF:**
13 growth factor; **GFP:** green fluorescent protein; **HA:** hyaluronic acid (or hyaluronan); **HAB:** high
14 affinity binding; **hACs:** human articular chondrocytes; **HAP:** hydroxyapatite; **H&E:** hematoxylin
15 and eosin; **HUVECs:** human umbilical vein endothelial cells; **IC₅₀:** half inhibitory concentration;
16 **IL-1:** interleukin 1; **IL-10:** interleukin 10; **K_D:** dissociation constant; **LAB:** low affinity binding;
17 **MRI:** magnetic resonance imaging; **mRNA:** messenger RNA; **MSCs:** mesenchymal stem cells;
18 **mTNF- α :** murine TNF- α ; **NGS:** next generation sequencing; **NLS:** nuclear localization signal;
19 **NPCs:** neural progenitor cells; **NSCs:** neural stem cells; **OA:** osteoarthritis; **ODM:** osteogenic
20 differentiation medium; **PA:** peptide amphiphile; **PAMAM:** poly(amido)amine; **PCL:**
21 polycaprolactone; **pDNA:** plasmid DNA; **PEG:** polyethyleneglycol **PEI:** polyethyleneimine; **PET:**
22 positron emission tomography; **PMEF:** primary mouse embryonic fibroblast; **QDs:** quantum-
23 dots; **RGD:** arginine-glycine-aspartic acid; **rhBMP-2:** recombinant form of human BMP-2; **RM:**
24 regenerative medicine; **RHAMM:** receptor for hyaluronan-mediated motility; **rMSC:** rat MSCs;
25 **RNA:** ribonucleic acid; **RNAi:** RNA interference; **S2P:** stabilin-2 peptide; **SA:** streptavidin; **SAM:**
26 self-assembled monolayer; **SEM:** scanning electron microscopy; **siRNA:** small interfering RNA;
27 **SPACE:** skin permeating and cell entering; **ss:** single stranded; **TGF- β R:** transforming growth
28 factor β receptor; **TGF- β :** transforming growth factor β ; **TNF:** tumor necrosis factor; **VCAM-1:**
29 vascular cell adhesion molecule 1; **VNP:** VHSPNKK-modified magnetofluorescent nanoparticle.
30
31
32
33
34
35
36
37

38 ASSOCIATED CONTENT

39 Supporting Information

40 Table S1 shows the follow-up analysis on the subsequent applications of peptide sequences
41 listed in Table 1. This material is available free of charge *via* the Internet at <http://pubs.acs.org>.
42
43

44 REFERENCES

- 45
46
47 1. Mason, C., and Dunnill, P. (2008) A brief definition of regenerative medicine, *Regen*
48 *Med* 3, 1-5.
49 2. Smith, G. P. (1985) Filamentous fusion phage: novel expression vectors that display
50 cloned antigens on the virion surface, *Science* 228, 1315-1317.
51 3. Deutscher, S. L. (2010) Phage display in molecular imaging and diagnosis of cancer,
52 *Chem Rev* 110, 3196-3211.
53 4. Hamzeh-Mivehroud, M., Alizadeh, A. A., Morris, M. B., Church, W. B., and Dastmalchi,
54 S. (2013) Phage display as a technology delivering on the promise of peptide drug
55 discovery, *Drug Discov Today* 18, 1144-1157.
56 5. Krumpke, L. R., and Mori, T. (2006) The Use of Phage-Displayed Peptide Libraries to
57 Develop Tumor-Targeting Drugs, *Int J Pept Res Ther* 12, 79-91.
58
59
60

- 1
 - 2
 - 3
 - 4
 - 5
 - 6
 - 7
 - 8
 - 9
 - 10
 - 11
 - 12
 - 13
 - 14
 - 15
 - 16
 - 17
 - 18
 - 19
 - 20
 - 21
 - 22
 - 23
 - 24
 - 25
 - 26
 - 27
 - 28
 - 29
 - 30
 - 31
 - 32
 - 33
 - 34
 - 35
 - 36
 - 37
 - 38
 - 39
 - 40
 - 41
 - 42
 - 43
 - 44
 - 45
 - 46
 - 47
 - 48
 - 49
 - 50
 - 51
 - 52
 - 53
 - 54
 - 55
 - 56
 - 57
 - 58
 - 59
 - 60
6. Smith, G. P., and Petrenko, V. A. (1997) Phage Display, *Chem Rev* 97, 391-410.
 7. Petrenko, V. (2008) Evolution of phage display: from bioactive peptides to bioselective nanomaterials, *Expert Opin Drug Deliv* 5, 825-836.
 8. Shiba, K. (2010) Exploitation of peptide motif sequences and their use in nanobiotechnology, *Curr Opin Biotechnol* 21, 412-425.
 9. Wilson, D. R., and Finlay, B. B. (1998) Phage display: applications, innovations, and issues in phage and host biology, *Can J Microbiol* 44, 313-329.
 10. Bratkovic, T. (2010) Progress in phage display: evolution of the technique and its application, *Cell Mol Life Sci* 67, 749-767.
 11. Pande, J., Szewczyk, M. M., and Grover, A. K. (2010) Phage display: concept, innovations, applications and future, *Biotechnol Adv* 28, 849-858.
 12. Paschke, M. (2006) Phage display systems and their applications, *Appl Microbiol Biotechnol* 70, 2-11.
 13. Sergeeva, A., Kolonin, M. G., Mollrem, J. J., Pasqualini, R., and Arap, W. (2006) Display technologies: application for the discovery of drug and gene delivery agents, *Adv Drug Deliv Rev* 58, 1622-1654.
 14. Smothers, J. F., Henikoff, S., and Carter, P. (2002) Tech.Sight. Phage display. Affinity selection from biological libraries, *Science* 298, 621-622.
 15. Barbas, C. F., Burton, D. R., Scott, J. K., and Silverman, G. J. (2001) *Phage Display: A Laboratory Manual*, Cold Spring Harbor Laboratory Press, New York.
 16. Clarkson, T., and Lowman, H. B. (2004) *Phage Display: A Practical Approach*, Oxford University Press, Oxford.
 17. Hamilton, P. T., Jansen, M. S., Ganesan, S., Benson, R. E., Hyde-Deruyser, R., Beyer, W. F., Gile, J. C., Nair, S. A., Hodges, J. A., and Gron, H. (2013) Improved bone morphogenetic protein-2 retention in an injectable collagen matrix using bifunctional peptides, *PLoS One* 8, e70715.
 18. Bastings, M. M., Helms, B. A., van Baal, I., Hackeng, T. M., Merckx, M., and Meijer, E. W. (2011) From phage display to dendrimer display: insights into multivalent binding, *J Am Chem Soc* 133, 6636-6641.
 19. Hajduczki, A., Majumdar, S., Fricke, M., Brown, I. A., and Weiss, G. A. (2011) Solubilization of a membrane protein by combinatorial supercharging, *ACS Chem Biol* 6, 301-307.
 20. Giordano, R. J., Cardo-Vila, M., Lahdenranta, J., Pasqualini, R., and Arap, W. (2001) Biopanning and rapid analysis of selective interactive ligands, *Nat Med* 7, 1249-1253.
 21. Derda, R., Musah, S., Orner, B. P., Klim, J. R., Li, L., and Kiessling, L. L. (2010) High-throughput discovery of synthetic surfaces that support proliferation of pluripotent cells, *J Am Chem Soc* 132, 1289-1295.
 22. Arap, W., Kolonin, M. G., Trepel, M., Lahdenranta, J., Cardo-Vila, M., Giordano, R. J., Mintz, P. J., Ardelt, P. U., Yao, V. J., Vidal, C. I., Chen, L., Flamm, A., Valtanen, H., Weavind, L. M., Hicks, M. E., Pollock, R. E., Botz, G. H., Bucana, C. D., Koivunen, E., Cahill, D., Troncoso, P., Baggerly, K. A., Pentz, R. D., Do, K. A., Logothetis, C. J., and Pasqualini, R. (2002) Steps toward mapping the human vasculature by phage display, *Nat Med* 8, 121-127.
 23. Chen, Y., Shen, Y., Guo, X., Zhang, C., Yang, W., Ma, M., Liu, S., Zhang, M., and Wen, L. P. (2006) Transdermal protein delivery by a coadministered peptide identified via phage display, *Nat Biotechnol* 24, 455-460.
 24. Pasqualini, R., and Ruoslahti, E. (1996) Organ targeting in vivo using phage display peptide libraries, *Nature* 380, 364-366.
 25. Trepel, M., Arap, W., and Pasqualini, R. (2002) In vivo phage display and vascular heterogeneity: implications for targeted medicine, *Curr Opin Chem Biol* 6, 399-404.
 26. Nowakowski, G. S., Dooner, M. S., Valinski, H. M., Mihaliak, A. M., Quesenberry, P. J., and Becker, P. S. (2004) A specific heptapeptide from a phage display peptide library

- homes to bone marrow and binds to primitive hematopoietic stem cells, *Stem Cells* 22, 1030-1038.
27. Matochko, W. L., Chu, K., Jin, B., Lee, S. W., Whitesides, G. M., and Derda, R. (2012) Deep sequencing analysis of phage libraries using Illumina platform, *Methods* 58, 47-55.
28. Hoen, P. A., Jirka, S. M., Ten Broeke, B. R., Schultes, E. A., Aguilera, B., Pang, K. H., Heemskerk, H., Aartsma-Rus, A., van Ommen, G. J., and den Dunnen, J. T. (2012) Phage display screening without repetitious selection rounds, *Anal Biochem* 421, 622-631.
29. Ernst, A., Gfeller, D., Kan, Z., Seshagiri, S., Kim, P. M., Bader, G. D., and Sidhu, S. S. (2010) Coevolution of PDZ domain-ligand interactions analyzed by high-throughput phage display and deep sequencing, *Mol Biosyst* 6, 1782-1790.
30. Rentero Rebollo, I., Sabisz, M., Baeriswyl, V., and Heinis, C. (2014) Identification of target-binding peptide motifs by high-throughput sequencing of phage-selected peptides, *Nucleic Acids Res* 42, e169.
31. Robins, W. P., Faruque, S. M., and Mekalanos, J. J. (2013) Coupling mutagenesis and parallel deep sequencing to probe essential residues in a genome or gene, *Proc Natl Acad Sci U S A* 110, E848-857.
32. Zhang, H., Torkamani, A., Jones, T. M., Ruiz, D. I., Pons, J., and Lerner, R. A. (2011) Phenotype-information-phenotype cycle for deconvolution of combinatorial antibody libraries selected against complex systems, *Proc Natl Acad Sci U S A* 108, 13456-13461.
33. Huang, J., Ru, B., and Dai, P. (2011) Bioinformatics resources and tools for phage display, *Molecules* 16, 694-709.
34. Huang, J., Ru, B., Zhu, P., Nie, F., Yang, J., Wang, X., Dai, P., Lin, H., Guo, F. B., and Rao, N. (2012) MimoDB 2.0: a mimotope database and beyond, *Nucleic Acids Res* 40, 271-277.
35. Sahu, A., Kay, B. K., and Lambris, J. D. (1996) Inhibition of human complement by a C3-binding peptide isolated from a phage-displayed random peptide library, *J Immunol* 157, 884-891.
36. Ricklin, D., and Lambris, J. D. (2008) Compstatin: a complement inhibitor on its way to clinical application, *Adv Exp Med Biol* 632, 273-292.
37. Nilsson, B., Ekdahl, K. N., Mollnes, T. E., and Lambris, J. D. (2007) The role of complement in biomaterial-induced inflammation, *Mol Immunol* 44, 82-94.
38. Helms, B. A., Reulen, S. W., Nijhuis, S., de Graaf-Heuvelmans, P. T., Merckx, M., and Meijer, E. W. (2009) High-affinity peptide-based collagen targeting using synthetic phage mimics: from phage display to dendrimer display, *J Am Chem Soc* 131, 11683-11685.
39. Gron, H., and Duffin, D. (2008) Methods and compositions for promoting localization of pharmaceutically active agents to bone, US 2008/0268015 A1, United States. Patent 2008/0268015 A1.
40. Rothenfluh, D. A., Bermudez, H., O'Neil, C. P., and Hubbell, J. A. (2008) Biofunctional polymer nanoparticles for intra-articular targeting and retention in cartilage, *Nat Mater* 7, 248-254.
41. Chan, J. M., Zhang, L., Tong, R., Ghosh, D., Gao, W., Liao, G., Yuet, K. P., Gray, D., Rhee, J. W., Cheng, J., Golomb, G., Libby, P., Langer, R., and Farokhzad, O. C. (2010) Spatiotemporal controlled delivery of nanoparticles to injured vasculature, *Proc Natl Acad Sci U S A* 107, 2213-2218.
42. Mummert, M. E., Mohamadzadeh, M., Mummert, D. I., Mizumoto, N., and Takashima, A. (2000) Development of a peptide inhibitor of hyaluronan-mediated leukocyte trafficking, *J Exp Med* 192, 769-779.
43. Roy, M. D., Stanley, S. K., Amis, E. J., and Becker, M. L. (2008) Identification of a highly specific hydroxyapatite-binding peptide using phage display, *Adv Mater* 20, 1830-1836.

- 1
2
3 44. Gungormus, M., Fong, H., Kim, I. W., Evans, J. S., Tamerler, C., and Sarikaya, M. (2008) Regulation of in vitro calcium phosphate mineralization by combinatorially selected hydroxyapatite-binding peptides, *Biomacromolecules* 9, 966-973.
- 4
5
6 45. Chung, W. J., Kwon, K. Y., Song, J., and Lee, S. W. (2011) Evolutionary screening of collagen-like peptides that nucleate hydroxyapatite crystals, *Langmuir* 27, 7620-7628.
- 7
8 46. Li, Z., Fan, J., Zhao, W., Jin, L., and Ma, L. (2011) The specific binding of peptide ligands to cardiomyocytes derived from mouse embryonic stem cells, *J Pept Sci* 17, 771-782.
- 9
10 47. Cheung, C. S., Lui, J. C., and Baron, J. (2013) Identification of chondrocyte-binding peptides by phage display, *J Orthop Res* 31, 1053-1058.
- 11
12 48. Pi, Y., Zhang, X., Shi, J., Zhu, J., Chen, W., Zhang, C., Gao, W., Zhou, C., and Ao, Y. (2011) Targeted delivery of non-viral vectors to cartilage in vivo using a chondrocyte-homing peptide identified by phage display, *Biomaterials* 32, 6324-6332.
- 13
14
15 49. Nie, J., Chang, B., Traktuev, D. O., Sun, J., March, K., Chan, L., Sage, E. H., Pasqualini, R., Arap, W., and Kolonin, M. G. (2008) IFATS collection: Combinatorial peptides identify alpha5beta1 integrin as a receptor for the matricellular protein SPARC on adipose stromal cells, *Stem Cells* 26, 2735-2745.
- 16
17
18 50. Daquinag, A. C., Zhang, Y., Amaya-Manzanares, F., Simmons, P. J., and Kolonin, M. G. (2011) An isoform of decorin is a resistin receptor on the surface of adipose progenitor cells, *Cell Stem Cell* 9, 74-86.
- 19
20
21 51. Shao, Z., Zhang, X., Pi, Y., Wang, X., Jia, Z., Zhu, J., Dai, L., Chen, W., Yin, L., Chen, H., Zhou, C., and Ao, Y. (2012) Polycaprolactone electrospun mesh conjugated with an MSC affinity peptide for MSC homing in vivo, *Biomaterials* 33, 3375-3387.
- 22
23
24 52. Balian, G. (2008) Bone Targeting Peptides, United States. Patent 7,323,542.
- 25
26
27 53. Ma, K., Wang, D. D., Lin, Y., Wang, J., Petrenko, V., and Mao, C. (2013) Synergetic Targeted Delivery of Sleeping-B Beauty Transposon System to Mesenchymal Stem Cells Using LPD Nanoparticles Modified with a Phage-Displayed Targeting Peptide, *Adv Funct Mater* 23, 1172-1181.
- 28
29
30 54. Zhao, W., Jin, L., Yuan, H., Tan, Z., Zhou, C., Li, L. S., and Ma, L. (2013) Targeting human embryonic stem cells with quantum dot-conjugated phages, *Sci Rep* 3, 3134.
- 31
32
33 55. Zhao, S., Zhao, W., and Ma, L. (2010) Novel peptide ligands that bind specifically to mouse embryonic stem cells, *Peptides* 31, 2027-2034.
- 34
35
36 56. Lu, S., Xu, X., Zhao, W., Wu, W., Yuan, H., Shen, H., Zhou, C., Li, L. S., and Ma, L. (2010) Targeting of embryonic stem cells by peptide-conjugated quantum dots, *PLoS One* 5, 1-10.
- 37
38
39 57. Schmidt, A., Haas, S. J., Hildebrandt, S., Scheibe, J., Eckhoff, B., Racek, T., Kempermann, G., Wree, A., and Putzer, B. M. (2007) Selective targeting of adenoviral vectors to neural precursor cells in the hippocampus of adult mice: new prospects for in situ gene therapy, *Stem Cells* 25, 2910-2918.
- 40
41
42 58. Caprini, A., Silva, D., Zanoni, I., Cunha, C., Volonte, C., Vescovi, A., and Gelain, F. (2013) A novel bioactive peptide: assessing its activity over murine neural stem cells and its potential for neural tissue engineering, *N Biotechnol* 30, 552-562.
- 43
44
45 59. Zhao, W., Yuan, H., Xu, X., and Ma, L. (2010) Isolation and initial application of a novel peptide that specifically recognizes the neural stem cells derived from rhesus monkey embryonic stem cells, *J Biomol Screen* 15, 687-694.
- 46
47
48 60. Hsu, T., and Mitragotri, S. (2011) Delivery of siRNA and other macromolecules into skin and cells using a peptide enhancer, *Proc Natl Acad Sci U S A* 108, 15816-15821.
- 49
50
51 61. Rangel, R., Guzman-Rojas, L., le Roux, L. G., Staquicini, F. I., Hosoya, H., Barbu, E. M., Ozawa, M. G., Nie, J., Jr, K. D., Langley, R. R., Sage, E. H., Koivunen, E., Gelovani, J. G., Lobb, R. R., Sidman, R. L., Pasqualini, R., and Arap, W. (2012) Combinatorial targeting and discovery of ligand-receptors in organelles of mammalian cells, *Nat Commun* 3, 788.
- 52
53
54
55
56
57
58
59
60

- 1
2
3
4
5
6
7
8
9
10
11
12
13
14
15
16
17
18
19
20
21
22
23
24
25
26
27
28
29
30
31
32
33
34
35
36
37
38
39
40
41
42
43
44
45
46
47
48
49
50
51
52
53
54
55
56
57
58
59
60
62. Behanna, H. A., Donners, J. J., Gordon, A. C., and Stupp, S. I. (2005) Coassembly of amphiphiles with opposite peptide polarities into nanofibers, *J Am Chem Soc* **127**, 1193-1200.
63. Yayon, A., Aviezer, D., Safran, M., Gross, J. L., Heldman, Y., Cabilly, S., Givol, D., and Katchalski-Katzir, E. (1993) Isolation of peptides that inhibit binding of basic fibroblast growth factor to its receptor from a random phage-epitope library, *Proc Natl Acad Sci U S A* **90**, 10643-10647.
64. Lee, G. Y., Kim, J. H., Oh, G. T., Lee, B. H., Kwon, I. C., and Kim, I. S. (2011) Molecular targeting of atherosclerotic plaques by a stabilin-2-specific peptide ligand, *J Control Release* **155**, 211-217.
65. Li, L., Orner, B. P., Huang, T., Hinck, A. P., and Kiessling, L. L. (2010) Peptide ligands that use a novel binding site to target both TGF-beta receptors, *Mol Biosyst* **6**, 2392-2402.
66. Michon, I. N., Penning, L. C., Molenaar, T. J., van Berkel, T. J., Biessen, E. A., and Kuiper, J. (2002) The effect of TGF-beta receptor binding peptides on smooth muscle cells, *Biochem Biophys Res Commun* **293**, 1279-1286.
67. Kelly, K. A., Allport, J. R., Tsourkas, A., Shinde-Patil, V. R., Josephson, L., and Weissleder, R. (2005) Detection of vascular adhesion molecule-1 expression using a novel multimodal nanoparticle, *Circ Res* **96**, 327-336.
68. Nahrendorf, M., Jaffer, F. A., Kelly, K. A., Sosnovik, D. E., Aikawa, E., Libby, P., and Weissleder, R. (2006) Noninvasive vascular cell adhesion molecule-1 imaging identifies inflammatory activation of cells in atherosclerosis, *Circulation* **114**, 1504-1511.
69. Yang, B., Yang, B. L., Savani, R. C., and Turley, E. A. (1994) Identification of a common hyaluronan binding motif in the hyaluronan binding proteins RHAMM, CD44 and link protein, *Embo J* **13**, 286-296.
70. Chai, C., and Leong, K. W. (2007) Biomaterials approach to expand and direct differentiation of stem cells, *Mol Ther* **15**, 467-480.
71. Mallanna, S. K., and Rizzino, A. (2012) Systems biology provides new insights into the molecular mechanisms that control the fate of embryonic stem cells, *J Cell Physiol* **227**, 27-34.
72. Meirelles Lda, S., Fontes, A. M., Covas, D. T., and Caplan, A. I. (2009) Mechanisms involved in the therapeutic properties of mesenchymal stem cells, *Cytokine Growth Factor Rev* **20**, 419-427.
73. Oh, I. H., and Humphries, R. K. (2012) Concise review: Multidimensional regulation of the hematopoietic stem cell state, *Stem Cells* **30**, 82-88.
74. Balian, G., Beck, G., Madhu, V., Sikes, R., Cui, Q., Liang, H., and Bush, J. (2010) Peptides from phage display library modulate gene expression in mesenchymal cells and potentiate osteogenesis in uncortical bone defects, *J Vis Exp*.
75. Cao, F. Y., Yin, W. N., Fan, J. X., Zhuo, R. X., and Zhang, X. Z. (2015) A novel function of BMHP1 and cBMHP1 peptides to induce the osteogenic differentiation of mesenchymal stem cells, *Biomater Sci-Uk* **3**, 345-351.
76. Cabanas-Danes, J., Nicosia, C., Landman, E., Karperien, M., Huskens, J., and Jonkheijm, P. (2013) A fluorogenic monolayer to detect the co-immobilization of peptides that combine cartilage targeting and regeneration, *J Mater Chem B* **1**, 1903-1908.
77. Li, L., Klim, J. R., Derda, R., Courtney, A. H., and Kiessling, L. L. (2011) Spatial control of cell fate using synthetic surfaces to potentiate TGF-beta signaling, *Proc Natl Acad Sci U S A* **108**, 11745-11750.
78. Gungormus, M., Branco, M., Fong, H., Schneider, J. P., Tamerler, C., and Sarikaya, M. (2010) Self assembled bi-functional peptide hydrogels with biomineralization-directing peptides, *Biomaterials* **31**, 7266-7274.
79. Segvich, S. J., Smith, H. C., and Kohn, D. H. (2009) The adsorption of preferential binding peptides to apatite-based materials, *Biomaterials* **30**, 1287-1298.

- 1
2
3 80. Weiger, M. C., Park, J. J., Roy, M. D., Stafford, C. M., Karim, A., and Becker, M. L. (2010)
4 Quantification of the binding affinity of a specific hydroxyapatite binding peptide,
5 *Biomaterials* 31, 2955-2963.
- 6 81. Jin, H. E., Jang, J., Chung, J., Lee, H. J., Wang, E., Lee, S. W., and Chung, W. J. (2015)
7 Biomimetic Self-Templated Hierarchical Structures of Collagen-Like Peptide
8 Amphiphiles, *Nano Lett* 15, 7138-7145.
- 9 82. Cigognini, D., Silva, D., Paloppi, S., and Gelain, F. (2013) Evaluation of Mechanical
10 Properties and Therapeutic Effect of Injectable Self-Assembling Hydrogels for Spinal
11 Cord Injury, *Journal of Biomedical Nanotechnology* 9, 1-13.
- 12 83. Gelain, F., Bottai, D., Vescovi, A., and Zhang, S. (2006) Designer self-assembling peptide
13 nanofiber scaffolds for adult mouse neural stem cell 3-dimensional cultures, *PLoS One*
14 1, e119.
- 15 84. Gelain, F., Cigognini, D., Caprini, A., Silva, D., Colleoni, B., Donega, M., Antonini, S.,
16 Cohen, B. E., and Vescovi, A. (2012) New bioactive motifs and their use in
17 functionalized self-assembling peptides for NSC differentiation and neural tissue
18 engineering, *Nanoscale* 4, 2946-2957.
- 19 85. Gelain, F., Panseri, S., Antonini, S., Cunha, C., Donega, M., Lowery, J., Taraballi, F.,
20 Cerri, G., Montagna, M., Baldissera, F., and Vescovi, A. (2011) Transplantation of
21 nanostructured composite scaffolds results in the regeneration of chronically injured
22 spinal cords, *ACS Nano* 5, 227-236.
- 23 86. Gelain, F., Silva, D., Caprini, A., Taraballi, F., Natalello, A., Villa, O., Nam, K. T.,
24 Zuckermann, R. N., Doglia, S. M., and Vescovi, A. (2011) BMHP1-derived self-
25 assembling peptides: hierarchically assembled structures with self-healing propensity
26 and potential for tissue engineering applications, *ACS Nano* 5, 1845-1859.
- 27 87. Lee, S. S., Hsu, E. L., Mendoza, M., Ghodasra, J., Nickoli, M. S., Ashtekar, A., Polavarapu,
28 M., Babu, J., Riaz, R. M., Nicolas, J. D., Nelson, D., Hashmi, S. Z., Kaltz, S. R., Earhart, J.
29 S., Merk, B. R., McKee, J. S., Bairstow, S. F., Shah, R. N., Hsu, W. K., and Stupp, S. I.
30 (2015) Gel scaffolds of BMP-2-binding peptide amphiphile nanofibers for spinal
31 arthrodesis, *Adv Healthc Mater* 4, 131-141.
- 32 88. Lin, C. C., and Anseth, K. S. (2009) Controlling Affinity Binding with Peptide-
33 Functionalized Poly(ethylene glycol) Hydrogels, *Adv Funct Mater* 19, 2325.
- 34 89. Shah, R. N., Shah, N. A., Del Rosario Lim, M. M., Hsieh, C., Nuber, G., and Stupp, S. I.
35 (2010) Supramolecular design of self-assembling nanofibers for cartilage regeneration,
36 *Proc Natl Acad Sci U S A* 107, 3293-3298.
- 37 90. Rasmussen, U. B., Schreiber, V., Schultz, H., Mischler, F., and Schughart, K. (2002)
38 Tumor cell-targeting by phage-displayed peptides, *Cancer Gene Ther* 9, 606-612.
- 39 91. Svendsen, N., Walton, J. G., and Bradley, M. (2012) Peptides for cell-selective drug
40 delivery, *Trends Pharmacol Sci* 33, 186-192.
- 41 92. Barry, M. A., Dower, W. J., and Johnston, S. A. (1996) Toward cell-targeting gene
42 therapy vectors: selection of cell-binding peptides from random peptide-presenting
43 phage libraries, *Nat Med* 2, 299-305.
- 44 93. Santos, J. L., Pandita, D., Rodrigues, J., Pego, A. P., Granja, P. L., Balian, G., and Tomas,
45 H. (2010) Receptor-mediated gene delivery using PAMAM dendrimers conjugated with
46 peptides recognized by mesenchymal stem cells, *Mol Pharm* 7, 763-774.
- 47 94. Liang, C., Guo, B., Wu, H., Shao, N., Li, D., Liu, J., Dang, L., Wang, C., Li, H., Li, S., Lau, W.
48 K., Cao, Y., Yang, Z., Lu, C., He, X., Au, D. W., Pan, X., Zhang, B. T., Lu, C., Zhang, H., Yue,
49 K., Qian, A., Shang, P., Xu, J., Xiao, L., Bian, Z., Tan, W., Liang, Z., He, F., Zhang, L., Lu, A.,
50 and Zhang, G. (2015) Aptamer-functionalized lipid nanoparticles targeting osteoblasts
51 as a novel RNA interference-based bone anabolic strategy, *Nat Med* 21, 288-294.
- 52 95. Zhang, G., Guo, B., Wu, H., Tang, T., Zhang, B. T., Zheng, L., He, Y., Yang, Z., Pan, X.,
53 Chow, H., To, K., Li, Y., Li, D., Wang, X., Wang, Y., Lee, K., Hou, Z., Dong, N., Li, G.,
54 Leung, K., Hung, L., He, F., Zhang, L., and Qin, L. (2012) A delivery system targeting
55
56
57
58
59
60

- 1
2
3 bone formation surfaces to facilitate RNAi-based anabolic therapy, *Nat Med* 18, 307-
4 314.
- 5 96. Naumova, A. V., Modo, M., Moore, A., Murry, C. E., and Frank, J. A. (2014) Clinical
6 imaging in regenerative medicine, *Nat Biotechnol* 32, 804-818.
- 7 97. Molek, P., Strukelj, B., and Bratkovic, T. (2011) Peptide phage display as a tool for drug
8 discovery: targeting membrane receptors, *Molecules* 16, 857-887.
- 9 98. Solis, M. A., Chen, Y. H., Wong, T. Y., Bittencourt, V. Z., Lin, Y. C., and Huang, L. L.
10 (2012) Hyaluronan regulates cell behavior: a potential niche matrix for stem cells,
11 *Biochem Res Int* 2012, 346972.
- 12 99. Volk, S. W., Iqbal, S. A., and Bayat, A. (2013) Interactions of the Extracellular Matrix
13 and Progenitor Cells in Cutaneous Wound Healing, *Advances in wound care* 2, 261-272.
- 14 100. Gray, B. P., and Brown, K. C. (2014) Combinatorial peptide libraries: mining for cell-
15 binding peptides, *Chem Rev* 114, 1020-1081.
- 16 101. Cao, L., Li, B., Yi, P., Zhang, H., Dai, J., Tan, B., and Deng, Z. (2014) The interplay of T1-
17 and T2-relaxation on T1-weighted MRI of hMSCs induced by Gd-DOTA-peptides,
18 *Biomaterials* 35, 4168-4174.
- 19 102. Barrow, M., Taylor, A., Murray, P., Rosseinsky, M. J., and Adams, D. J. (2015) Design
20 considerations for the synthesis of polymer coated iron oxide nanoparticles for stem
21 cell labelling and tracking using MRI, *Chem Soc Rev* 44, 6733-6748.
- 22 103. Taylor, A., Wilson, K. M., Murray, P., Fernig, D. G., and Levy, R. (2012) Long-term
23 tracking of cells using inorganic nanoparticles as contrast agents: are we there yet?,
24 *Chem Soc Rev* 41, 2707-2717.
- 25 104. Yea, K., Xie, J., Zhang, H., Zhang, W., and Lerner, R. A. (2015) Selection of multiple
26 agonist antibodies from intracellular combinatorial libraries reveals that cellular
27 receptors are functionally pleiotropic, *Curr Opin Chem Biol* 26, 1-7.
- 28
29
30
31
32
33
34
35
36
37
38
39
40
41
42
43
44
45
46
47
48
49
50
51
52
53
54
55
56
57
58
59
60